Cell Biochem Biophys (2013) 66:205–227
DOI 10.1007/s12013-012-9469-4

ORIGINAL PAPER

Angiostatic Properties of Sulindac and Celecoxib in the Experimentally Induced Inflammatory Colorectal Cancer

Vivek Vaish · Honit Piplani · Chandan Rana · Sankar Nath Sanyal

Published online: 13 November 2012

Abstract Initiation of various cancers has been observed to be regulated via a prolonged inflammatory state in the tissues. However, molecular role of such a localized inflammation is not clear in the advanced stages of colorectal cancer. In this study, we have elaborated the role of various pro- and anti-inflammatory cytokines, transcription, and angiogenic factors in the progression of the 1,2-dimethylhydrazine dihydrochloride (DMH)-induced late phage colorectal cancer and also observed the chemopreventive role of the two non-steroidal anti-inflammatory drugs (NSAIDs), viz., Sulindac and Celecoxib. Carcinogenic changes were observed with morphological and histopathological studies, whereas mRNA and protein regulations of various biomolecules were identified via RT- or qRT-PCR, western blot and immunofluorescence analysis, respectively. Activity of inducible nitric oxide (NO) and cyclooxygenase-2 enzymes were analyzed using standard NO assay and prostaglandin E_2 immunoassay, whereas activities of matrix metalloproteinases (MMP-2 and-9) were identified by gelatin zymography. Flowcytometry was performed for the relative quantification of the apoptotic events. Molecular docking studies of Sulindac and Celecoxib were also performed with different target proteins to observe their putative mechanisms of action. As a result, we found that DMH-treated animals were having over-expression of various pro-inflammatory cytokines (IL-1β, IL-2, and IFNγ), aberrant nuclear localization of activated cell survival transcription factors (NF-κB and Stat3) along with the increased incidence of activated angiogenic factors (MMP-2 and MMP-9) suggesting a marked role of inflammation in the tumor progression. However, NSAIDs co-administration has significantly reduced the angiogenic potential of the growing neoplasm.

Keywords Angiogenesis · Chronic inflammation · Colorectal cancer · Cyclooxygenase-2 · Gelatin zymography · Matix metalloproteinases · Molecular docking

Introduction

Contrary to beneficial acute inflammation, chronic inflammation has been linked with the development of various malignancies where prolonged localized inflammatory condition may give rise to the increased cell survival, proliferation, suppression of apoptosis, invasion, angiogenesis, and metastasis [1]. In a solid tumor microenvironment, tumor cells and host cells interact with each other via secreted growth factors and cytokines (autocrine) which might indirectly affect the nearby stromal and endothelial cells (paracrine) to promote neovascularization. A solid tumor would not be able to survive more than 2–3 mm^3 without an adequate supply of oxygen and nutrients [2]. Various pro-inflammatory cytokines and chemokines have earlier been reported to be involved in turning "on" the angiogenic switch via the activation of downstream signaling molecules [3].

Reports on inflammatory diseases and various human cancers show higher levels of prostaglandins (PGs) which are synthesized by cyclooxygenase (COX) enzyme. COX has two isoforms: COX-1 and COX-2, while COX-1 serves

Electronic supplementary material The online version of this article (doi:10.1007/s12013-012-9469-4) contains supplementary material, which is available to authorized users.

V. Vaish · H. Piplani · C. Rana · S. N. Sanyal (✉)
Department of Biophysics, Panjab University, Chandigarh 160 014, India
e-mail: sanyalpu@gmail.com

as a homeostatic or house-keeping enzyme and is ubiquitously present among the healthy cells; COX-2, however, is predominantly observed in higher proportions during inflammation and malignancies [4]. Higher expression and activation of COX-2 and thereby produced PGs especially prostaglandin E_2 (PGE_2) has been documented to play an important role in promoting angiogenesis via vascular endothelial growth factor (VEGF) [1]. Interleukin-1β (IL-1β) which is a pro-inflammatory cytokine has also been observed to induce VEGF expression but via COX-2-independent mechanism [5]. However, as observed earlier, IL-1β and COX-2 positively regulate each other during inflammation and carcinogenesis [6, 7] but they might follow different signaling pathways to induce the same target molecule VEGF.

Co-operation of other pro-inflammatory cytokines (e.g., IL-2) also protects the tumor cells for being recognized as non-self by the cytotoxic lymphocytes as IL-2 causes activation-induced cell death (AICD) in those activated cytotoxic lymphocytes [8]. Autocrine and paracrine signaling of such pro-inflammatory cytokines is involved in the various intracellular downstream cell survival pathways which include nuclear localization of transcription factors, anti-apoptotic proteins, and angiogenic factors [9]. Along with cytokines, chemokines also play an important role in the consistency of localized inflammation via regulating the recruitment and trafficking of leukocytes inside the inflamed tissue [3]. Based on the position of their key cysteine residues, chemokines are grouped in four classes: C, CC, CXC, and CX3C [1]. Previously, we have reported the two antagonistic CC group chemokines, viz., monocyte chemotactic protein-1 (MCP-1 or CCL2) which was observed to be up-regulated during tumorigenesis while macrophage inflammatory protein-1β (MIP-1β or CCL4) which was positively regulated by diclofenac administration for the suppression of tumor growth [10]. However, still there is nothing much clear about the composite effects of these pro- and anti-inflammatory cytokines and chemokines on the progression of colorectal cancer which has become a leading cause of mortality worldwide due to poor prognosis.

It is thought that chemoprevention of colorectal cancer could be achieved in two ways either via suppressing the localized inflammation or by regulating the neovascularization. In the past few decades, non-steroidal anti-inflammatory drugs (NSAIDs) have shown promising anti-tumor effects in relation to colorectal cancer and hence US Food and Drug Administration (FDA) has approved Sulindac (COX non-specific) and Celecoxib (COX-2-specific) for the cure of patients suffering from hereditary non-polyposis colorectal cancer (HNPCC) [11]. In our previous studies, we have also reported the mechanisms of anti-neoplastic actions of these two drugs in the experimental model of colorectal cancer [12–14].

In this study, we investigated the angiostatic role of Sulindac and Celecoxib in the advanced stage of experimental colorectal cancer which could be mediated via the regulation of various pro- and anti-inflammatory cytokines [e.g., IL-1β, IL-2, IL-4, interferon-(IFN)-γ, and tumor necrosis factor-(TNF)-α], CC chemokines (MCP-1 and MIP-1β), transcription factors (nuclear factor-κB or NF-κB, signal transducer and activator of transcription 3 or Stat3 and peroxisome proliferator-activated receptor-γ or PPARγ) and angiogenic agents (VEGF-A, matrix metalloproteinases-2 or MMP-2, MMP-9 and inducible nitric oxide synthase or iNOS). To get further insight into the anti-inflammatory and angiostatic role of these NSAIDs, molecular interactions were observed using GLIDE software from Schrödinger Suite 2011, USA programme through flexible molecular docking of these NSAIDs with different inflammatory/angiogenic factors and their receptors.

Materials and Methods

Chemicals

1,2-Dimethylhydrazine dihydrochloride (DMH), Sulindac and Bradford reagent were purchased from Sigma-Aldrich (St. Louis, MO, USA). Celecoxib was a generous gift from Ranbaxy Pharmaceuticals Ltd. (Gurgaon, India). Prostaglandin E_2 Enzyme Immunoassay Kit was purchased from Enzo Life Sciences, Exeter, UK. Multi-parameter Apoptosis Assay Kit was purchased from Cayman Chemical Company, Ann Arbor, USA. Primary antibodies were purchased from Santa Cruz Biotechnology (CA, USA) and BD Biosciences (CA, USA). Alkaline phosphatase-conjugated secondary antibodies, fluorescein isothiocyanate (FITC)-conjugated secondary antibodies, and BCIP-NBT were purchased from Genei (Bangalore, India). FITC-conjugated-CD4 and phycoerythrin (PE)-conjugated CD8 monoclonal antibodies were a generous gift from Department of Biochemistry, Panjab University, Chandigarh. All other chemicals and reagents used in this study were of analytical grade and purchased from Himedia (Mumbai, India).

Animal Procurement

Male Sprague–Dawley rats of body weight between 150 and 200 g were obtained from the Central Animal House, Panjab University after the approval of the present protocol by the Ethics Committee of Animal Care. They were acclimatized and given rodent chow and water ad libitum for at least 1 week. They were maintained as per the principles and guidelines of the Committee for the Purpose of Control and Supervision on Experiments on Animals

(CPCSEA), Ministry of Environment Science and Forests, Govt. of India. They were housed three per cage in polypropylene cages with a wire mesh top and a hygienic bed of husk (regularly changed) in a well-ventilated animal room. The animals were also maintained at the ambient temperature and humidity, and under a 12-h photoperiod of light and darkness, respectively.

Treatment Schedule

Animals were assorted into the following groups:

Control Group, Vehicle Treated

Animals were administered the vehicle (1 mM EDTA-saline subcutaneously (s.c.) in weekly injection and 0.5 % carboxymethyl cellulose sodium salt (CMC) per oral (p.o.) daily [12–14].

1,2-Dimethylhydrazine Dihydrochloride (DMH) Group

Animals were administered with DMH weekly at a dose of 30 mg/kg body weight (s.c.). The dose of DMH has been established in our laboratory earlier [12–14]. DMH was freshly prepared in 1 mM EDTA–saline, pH adjusted to 7 using dilute 1 M NaOH solution.

DMH + Sulindac Group

Sulindac was given daily p.o. within its therapeutic anti-inflammatory dose (ED_{50} for rats, 20 mg/kg body weight) to the animals along with the weekly administration of 30 mg/kg body weight of DMH [14–16].

DMH + Celecoxib Group

Celecoxib was administered p.o. daily (ED_{50} for rats, 6 mg/kg body weight) to the animals along with the weekly administration of 30 mg/kg body weight of DMH [12–16].

After 18 weeks, animals were kept on overnight fasting with drinking water ad libitum and killed the next day under an over anesthesia with ether. The animal body weights in all the groups were recorded once in a week.

Gross Morphology

The colons were removed and flushed clear with ice-cold physiological saline (NaCl solution, 9 g/L). These were opened longitudinally along the median and laid flat to examine the incidence of tumors and macroscopic neoplastic lesions/plaques called the multiple plaque lesions (MPLs). The colons were divided into proximal, medial, and distal segments.

Histopathology

Colon pieces were removed from the killed rats and immediately fixed in 10 % buffered formalin for 24 h. The tissues were embedded in wax and 3–5-μm-thick sections were cut using a hand-driven microtome and transferred to the poly-L-lysine coated slides [13]. Sections were dewaxed in mixed xylenes, and standard staining procedures were performed to stain the sections with mucicarmine, alcian blue and periodic acid-schiff (PAS) stain. Slides were mounted in DPX, viewed under a light microscope (×100) and photographed.

Isolation of Colonocytes

Colonocytes were obtained from the freshly isolated colons by the method of Mouillé et al. [17], as described earlier [14, 15]. Trypan blue dye exclusion was performed each time for every group of isolated colonocytes and the viability of cells observed ~90 %.

Apoptosis Assay

The assay kit for the apoptotic events contained four different agents: (a) Annexin V-FITC (to detect the externalized phosphatidylserine residues of plasma membrane), (b) tetramethylrhodamine ethyl ester (TMRE, to detect the differential mitochondrial potential), (c) hoechst dye (to differentiate between the nuclear morphologies of live and apoptotic cells), (d) 7-aminoactinomycin D dye (7-AAD, to differentiate between live, apoptotic and dead cells). Out of these components only Annexin V-FITC and 7-AAD were further utilized to study the apoptotic potentials in a flowcytometer.

2×10^6 cells were taken and the staining procedure was followed according to the manufacture's protocol (Cayman Chemical Company, USA) for flow cytometry. Fluorescence of FITC and 7-AAD were detected in FL-1 and FL-3 channels, respectively (electronic compensation was done to avoid major spillage of fluorescence into both the channels) in a BD FACSCalibur system along with the data acquisition and analysis in BD CellQuest Pro software.

Prostaglandin E_2 Enzyme Immunoassay

A competitive immunoassay was performed for the quantification of PGE_2 in colonic mucosa. The kit uses a monoclonal antibody to PGE_2 to bind, in a competitive manner, the PGE_2 in the sample, standard, or an alkaline phosphatase molecule which has PGE_2 covalently attached to it.

A 10 % homogenate was prepared from freshly isolated colonic tissues in ice-cold 1× PBS and cleared of cellular

debris by centrifugation at 1,000×*g* for 15 min at 4 °C. The supernatant obtained was again centrifuged at 10,000×*g* for 15 min at 4 °C. The clear supernatant was collected. The assay was performed according to the manufacturer's protocol using blank corrections, non-specific binding corrections and all the dilutions of the given PGE_2 standard. The plate was read at 405 nm in a STAT Fax 325 + strip type ELISA reader (Awareness Technology Inc., Palm City, FL, USA). PGE_2 concentrations were calculated according to the standard curve and expressed as picograms per milliliter.

Gelatin Zymography

For the study of matrix metalloproteinase activity as described earlier [10], a 10 % homogenate of colonic tissue was prepared in PBS followed by centrifugation at 1,000×*g* at 4 °C to remove the cellular debris. The supernatant was again centrifuged at 10,000×*g* at 4 °C and the resultant supernatant was subjected to gelatin zymography after estimation of protein by Bradford method [18]. Polyacrylamide minigels (12 %) were cast containing 0.1 % gelatin. Gelatin solution was made up to 2 % stock in distilled water and dissolved by heating. Equal amounts of samples (100-μg protein) were loaded in each lane in standard SDS loading buffer containing 0.1 % SDS without β-mercaptoethanol. Boiling was avoided before loading of the samples [19]. The gel was run at constant current of 15 mA, until the dye front reached the end of the gel. The gels were then soaked in 200 ml of 2.5 % (v/v) Triton X-100 in distilled water in a shaker for 1 h, with one change after 30 min at 20 °C to remove SDS. The gels were incubated in the incubation buffer (50 mM Tris, 200 mM NaCl, 10 mM $CaCl_2$, 0.05 % Nonidet-P40, pH 7.8) for 12 h at 37 °C and stained with Coomassie brilliant blue-R 250 in 50 % methanol and 10 % acetic acid, followed by washing with distilled water for 1 min. Gelatinolytic activities of MMP were detected as the clear zones of lysis against a blue background [19]. The gel was photographed with a Gel Doc (Fotodyne, Hartland, WI, USA) and analyzed using the Image J software (NIH, Bethesda, USA).

Western Blot

Protein samples/nuclear extracts (50 μg) were separated on 10 % SDS-PAGE. The separated proteins were electrophoretically transferred to nitrocellulose membrane (Millipore, Bangalore, India) and the transfer checked by staining with Ponceau S [11]. Immunoblot was prepared using primary antibodies (IL-1β: 1:1,000, IL-2: 1:1,000, IL-4: 1:1,000, IFNγ: 1:1,000, TNF-α: 1:500, iNOS: 1:500, Jak3: 1:1,000, Stat3: 2 μg/ml, IKKβ: 1:500, IκB: 1:500, NFκB: 1:500, PPARγ: 1:1,000, COX-1: 1:1,000, COX-2: 1:500, VEGF-A: 1:1,000, MMP-2: 1:1,000, MMP-9: 1:500, iNOS: 1:1,000, MCP-1: 1:500, MIP-1β: 1:1,000, and β-actin: 1:10,000) and alkaline phosphatase-conjugated respective IgG secondary antibodies. BCIP-NBT detection system was used to develop the blot. Bands obtained were analyzed using Image J software and the density expressed in gray values.

For preparation of cell lysates, colons were removed and rinsed. Total lysates were prepared in fresh ice-cold lysis buffer (10 mM Tris, 100 mM NaCl, 5 mM EDTA, 1 % Triton-X100, 1 mM PMSF, and 2 mM DTT, pH 8). The extracts were cleared by centrifugation at 10,000×*g* for 10 min at 4 °C and the supernatants collected.

For nuclear extract, the nuclei from the colonic tissues were suspended at 0–4 °C in 50 mM NaCl, 10 mM Hepes, pH 7.6, 0.1 mM EDTA, 25 % glycerol and 0.5 mM PMSF and pelleted by centrifugation in an Eppendorf centrifuge at 5,000×*g* for 15 min at 4 °C. Resulting nuclear debris was incubated in the same buffer for 30 min on ice, centrifuged at 10,000×*g* at 4 °C for 10 min and the resultant supernatant used as the nuclear extract. Protein concentration was determined by the method of Bradford (1976) [18].

iNOS Enzyme Activity

Estimation of Nitric Oxide (NO)

NO production was estimated by measuring nitrite, a stable metabolic product of NO, using Griess reagent [20]. To 100 μl of the sample, 100 μl of Griess reagent (1:1 ratio of 0.1 % *n*-naphthyl ethylenediamine dihydrochloride solution in distilled water and 1 % sulfanilamide in 2.5 % orthophosphoric acid) was added in an ELISA strip. The strip was incubated in dark for 10 min at room temperature; the pink color so observed was read for its absorbance at 540 nm in an ELISA reader. Concentrations were determined from a linear standard curve prepared using 10-mM stock solution of the sodium nitrite (1.25–10 nmol). The results were expressed as nanomoles of nitrite formed per milligram protein.

Estimation of L-Citrulline

The citrulline assay was based on its reaction with diacetylmonooxime and absorbance measured at 530 nm [21]. Reagent A (H_2SO_4, H_2O, H_3PO_4, $FeCl_3$), Reagent B (diacetyl monooxime, thiosemicarbazide), Reagent C (mix reagent A and B in 2:1 ratio), Reagent D (30 % $ZnSO_4$, 0.1 N HCl) were prepared. 40-μl sample was taken and 160-μl H_2O + 50-μl Reagent D added. The mixture was

centrifuged at 2,000 rpm for 10 min. 40-µl supernatant was taken and 480 µl of 0.1 N HCl and 1.5 ml of Reagent C added. The mixture was boiled for 5 min and OD was taken at 530 nm. Freshly made 1 mM L-citrulline in H_2O stock was taken to make standard dilutions. The amount of L-citrulline was calculated from the standard curve and values expressed as micromoles of L-citrulline formed per milligram protein.

Immunofluorescence

3–5-µm-thick paraffin sections were utilized for the immunofluorescence procedure [14, 15]. The sections were incubated in 1.5 % BSA with primary antibody of IL-1β (1:1,000), IL-2 (1:1,000), IL-4 (1:1,000), IFNγ (1:1,000), TNF-α (1:500), iNOS (1:500), CD4-FITC (1:500), CD8-PE (1:500), NF-κB (1:500), PPARγ (1:500), COX-2 (1:500), and VEGF-A (1:1,000) in a moist chamber for 2 h at 37 °C. For negative control, only 1.5 % BSA was added. After incubation, three washings were given with PBS, PBS Tween (PBS with 0.05 % Tween 20), and PBS, successively, for 5 min each. The sections were then incubated with the FITC-conjugated secondary antibody at a dilution of 1:10,000 for 2 h at 37 °C in dark. Sections were washed again in the same manner as described above, and all the sections except CD4-FITC and CD8-PE co-staining sections were counterstained with propidium iodide (PI) for 20 min at 37 °C in dark and washed as earlier. These were mounted in glycerol (1:10 in PBS), sealed with nail paint, and observed under a fluorescence microscope at ×400 (Axioscope A1, Zeiss, Germany), to which a digital camera (Jenoptik AG, Germany) is attached for photography.

mRNA Expression by Reverse Transcriptase-Polymerase Chain Reaction (RT-PCR) and Further Validation by Quantitative Real-Time-PCR (qRT-PCR)

Isolation of total RNA

Total RNA from colon tissues were isolated using HiPurA™ Total RNA Miniprep Purification Spin Kit from Himedia (Mumbai, India). Concentration, yield, and purity of the isolated RNA were analyzed by measuring the absorbance at 260, 280, and 320 nm in a spectrophotometer and calculating the ratios (A_{260}–A_{320}/A_{280}–A_{320}). The 320-nm absorbance was taken to correct the background absorbance.

$$\text{Concentration of RNA sample } (\mu g/ml) = 40 \times A_{260} \times \text{dilution factor.}$$

Further 1.2 % formaldehyde agarose gel electrophoresis was performed to check the quality of the isolated RNA.

Selection of Specific Pair of Primers

For RT-PCR and qRT-PCR, primers for IL-1β, TNF-α, MCP-1, MIP-1β were custom synthesized by Genei (Bangalore, India) and iNOS, IKKβ, IκB, NF-κB, PPARγ, VEGF-A, MMP-2, MMP-9, COX-1, COX-2, β-actin were by Metabion International AG (Martinsried, Germany). Primer sequences were chosen against the cDNA sequences using Primer-BLAST tool (NCBI). Details of accession numbers, primer sequences, and final product (amplicon) size are provided in Supplementary Table 1.

RT-PCR

RT-PCR was performed using Genei™ One step AMV RT-PCR kit in G-Storm GS482 thermal cycler (G-Storm Ltd. Somerset, UK) using specific set of primers. β-Actin analysis was done to rule out experimental errors. 2 µg of the total RNA was used for RT-PCR reaction. Reverse transcription reaction was set at 50 °C for 30 min and inactivation at 95 °C for 10 min followed by the cDNA amplification reaction of 35 cycles: 95 °C (denaturation) for 30 s, 55 °C (annealing) for 45 s, and 72 °C (extension) for 30 s. The products were finally incubated at 72 °C for 10 min to extend any incomplete single strand. Amplified cDNA products were analyzed by 2 % agarose gel electrophoresis and results presented via densitometric analysis of the bands using Image J software.

qRT-PCR

Validation of RT-PCR results was done by qRT-PCR using Precision OneStep™ qRT-PCR Mastermix with SYBR-green (PrimerDesign Ltd. Southampton, UK) in Roche LigthCycler® 480 System. The same reaction setup as described in RT-PCR method was used. β-Actin served as a reference gene for each triplicate set of reaction repeated three times. Results shown here are the mean normalized values of cDNA levels with the reference gene.

Molecular Docking

For molecular docking studies, various tools of Schrödinger Suit 2011 (USA) were utilized like as follows.

Ligand Preparation The 3-D crystal structures of Sulindac and Celecoxib were downloaded in .sdf format from Pubchem database. Ligand preparation was done using LigPrep Programme to minimize the energy and make the molecules stable.

Protein Preparation Co-crystallographic structures of interleukin-1 receptor type 1(PDB ID: 1G0Y), inducible

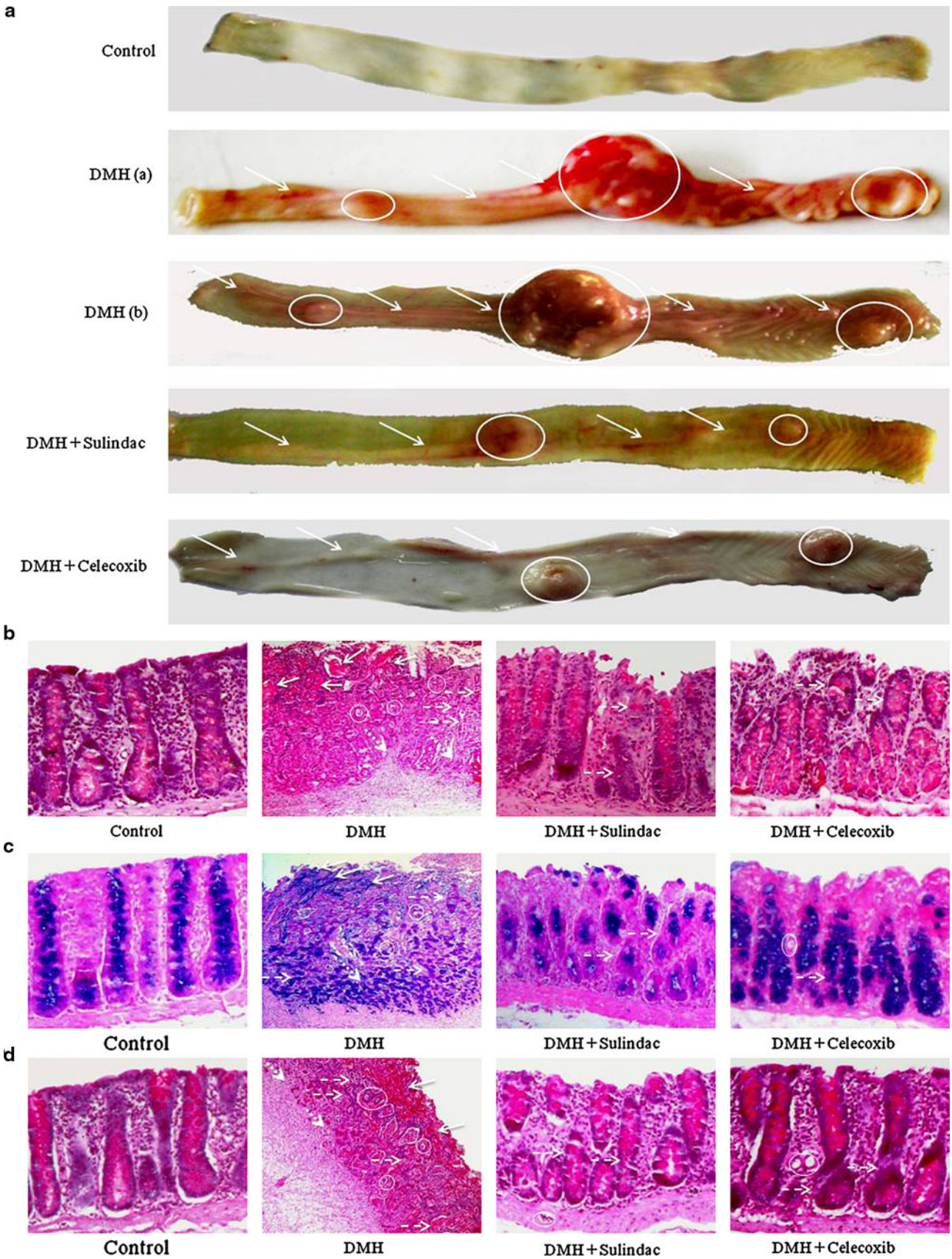
a
Control
DMH (a)
DMH (b)
DMH + Sulindac
DMH + Celecoxib
b
Control
DMH
DMH + Sulindac
DMH + Celecoxib
c
Control
DMH
DMH + Sulindac
DMH + Celecoxib
d
Control
DMH
DMH + Sulindac
DMH + Celecoxib

◀ **Fig. 1** **a** Morphological analysis of colons for tumor/MPLs incidence. Dissected colons from different groups were laid flat to examine the incidence of tumors and macroscopic neoplastic lesions/plaques also called the multiple plaque lesions or MPLs. DMH alone group: both DMH (a), unopened dissected colon, and DMH (b) longitudinally opened dissected colon, showing more number of tumors/MPLs (*circles*) along with the visible sign of aberrantly increased blood vasculature (*arrows*) running longitudinally across the colon and also connecting the tumors/MPLs. However, DMH + Sulindac and DMH + Celecoxib are having reduced number of tumors/MPLs (*circles*) along with a reduction in vasculature (*arrows*) as compared to the DMH. No such incidence of tumor/MPLs and aberrant blood vasculature were observed in the Control group. **b–d** Histopathological examination of colonic tissue sections by mucicarmine, alcian blue and periodic acid-Schiff (PAS) staining, respectively. **b** Mucicarmine staining reveals large pools of secreted acidic mucopolysaccharides (*arrows*) in the DMH group. **c** Alcian blue staining reveals the increased deposition of acidic sulfated mucopolysaccharides (*arrows*) secreted by the aberrant goblet cells in the DMH group. **d** PAS stain demonstrates the higher secretion of neutral mucopolysaccharides (*arrows*) by the malignant cells of the aberrant crypts in the DMH group. **b–d** Clear evidences of increased number in blood capillaries (*circles*), tumor invasiveness (*dotted arrows*), and largely dysplastic crypts (*broken arrows*) in the DMH group as compared to normal histoarchitecture of the Control group. However, DMH + Sulindac and DMH + Celecoxib groups seem to have an improved histoarchitecture with no incidence of abrupt mucin secretion

NO synthase (PDB ID: 3NQS), Jak3 (PDB ID: 1YVJ), Stat3 (PBD ID: 1BG1), VEGFR1 (PDB ID: 3HNG), and VGEFR2 (PDB ID: 1Y6A) were downloaded from Protein databank in .pdb format. Protein Preprep job was performed to remove redundant chains from all the co-crystallographic structures. All ligands/inhibitors and co-factors, except the active site ligand/inhibitor, were removed during protein structure refinement. All water molecules were removed, all hydrogen atoms were added and all atom force field (OPLS-2005) charges and atom types were assigned. Epik programme was used to generate different metal binding states and after choosing the best state for the co-crystallized ligand, energy minimization was done for the protein structure.

Grid Generation After energy minimization, grid for the active site was generated using GLIDE (Grid-Based Ligand Docking with Energetics) programme. Grids were prepared for each protein with the size of the bounding box set on 17 Å. The coordinates of the enclosing box were defined starting from the set of active site residues involved in hydrogen bonds with the co-crystallized ligand.

Docking Simulations After grid generation, molecular docking was performed between ligand molecules, Sulindac and Celecoxib, with protein molecules using GLIDE programme. GLIDE is based on the algorithm in which it starts searching with a rough positioning and scoring phase that significantly limits the search space and reduces the number of poses to be selected for minimization on the pre-computed OPLS-2005 van der Waals and electrostatic grids for the protein. The 5–10 lowest-energy poses obtained from this stage are then subjected to Monte Carlo simulations and the accepted minimized poses are rescored using the Glide Score function. This force field includes additional terms accounting for solvation and repulsive interactions. In order to provide a better correlation between good poses and good scores, Glide Extra-Precision (XP) Mode was subsequently used [22–24].

Statistical Analysis

Data were expressed as mean ± SD of four independent observations for each group. One-way analysis of variance (ANOVA) was done to compare the means between the different treatments using post-hoc comparison by least significant difference (LSD) method. The statistical software package SPSS v14 for windows was used for the purpose. A value of $p \leq 0.05$ was considered significant in this study.

Results

Morphological Analysis of Colon for Tumor/Lesion Incidence

Among the four groups, DMH alone showed higher incidence of tumors and lesions. In a representative Fig. 1a, DMH (a) shows the intact unopened colon bearing a full-grown tumor (circle) with excessive network of blood vessels in the middle section and two carcinogenic lesions (circles) on either side, i.e., proximal and distal. DMH (b) is the longitudinally opened colon of DMH (a) showing prominent continuous blood vessels (arrows) from proximal to distal part and passing through the lesions and full-grown tumor suggesting the evidence of angiogenesis. However, with the co-administration of Sulindac and Celecoxib the size and number of tumor/lesions (circles) reduced as compared to DMH group. DMH + Sulindac and DMH + Celecoxib groups also do not have many prominent blood vessels (arrows) as compared to DMH alone. No such incidence of tumor/lesions was observed in the control group.

Histopathological Examinations

Sections were observed after the staining with mucicarmine for acidic mucopolysaccharides (Fig. 1b), alcian blue for acidic sulfated mucopolysaccharides (Fig. 1c) and PAS stain for neutral mucopolysaccharides (Fig. 1d) at ×100 magnification. Mucicarmine, alcian blue, and PAS staining

Fig. 2 Immunomodulatory effects of Sulindac and Celecoxib for the regression of inflammation to prevent carcinogenesis. **a** Western blot analysis of pro-inflammatory cytokines IL-1β, IL-2, and IFNγ reveals their higher expression in the DMH group as compared to the control suggesting that persistence of localized inflammation could be a driving force for carcinogenesis in the colonic tissue. However, DMH + Sulindac and DMH + Celecoxib groups are having significantly lower expressions of these cytokines but significantly higher expressions of anti-inflammatory cytokines, i.e., IL-4 and TNF-α as compared to the DMH group which supports the anti-inflammatory nature of these drugs. A pro-inflammatory chemokine, i.e., MCP-1 which positively regulates the infiltration of neutrophils at the site of inflammation was also observed to be upregulated in the DMH group as compared to the control, whereas NSAIDs co-administration has not only significantly reduced its expression but also have enhanced the expression of an anti-inflammatory chemokine, MIP-1β. Higher expression of iNOS enzyme in DMH group also supports the occurrence of inflammation in the colon. β-Actin is serving as loading control. **b** Quantitative analysis of the blots normalized with β-actin in densitometric units. The values are mean ± SD of three independent experiments with four different animals from each group. $^{a}p \leq 0.05$, $^{b}p \leq 0.01$, and $^{c}p \leq 0.001$ in comparison to control, $^{y}p \leq 0.01$ and $^{z}p \leq 0.001$ in comparison to DMH by one way ANOVA. **c–e** Immunofluorescence analysis of pro-inflammatory cytokines, i.e., IL-1β, IL-2, and IFNγ, respectively, at ×400 showing higher expression and localization of these cytokines in the DMH group as compared to the control, whereas NSAIDs co-administration has downregulated the expression and thereby localization of those pro-inflammatory cytokines as compared to the DMH. **f**, **g** Immunofluorescence analysis of anti-inflammatory cytokines, i.e., IL-4 and TNF-α, respectively, at ×400 representing higher expression and localization (*arrows*) of these cytokines in DMH + Sulindac and DMH + Celecoxib groups as compared to the DMH group. **h** Immunofluorescence analysis of the marker enzyme for inflammation, i.e., iNOS in the colonic sections at ×400 showing higher expression and localization (*arrows*) of iNOS in the DMH-treated group as compared to the control. DMH + Sulindac and DMH + Celecoxib groups are having lower expression and thereby localization of iNOS as compared to the DMH group. **i** Immunofluorescence analysis of CD4+ T-cells and CD8+ T-cells at ×400 showing higher incidence of CD4+ T-cells (*dotted arrows*) in the DMH group, whereas DMH + Sulindac and DMH + Celecoxib groups show higher incidence of CD8+ T-cells (*arrows*) as compared to the DMH group. **j** mRNA levels of IL-1β, TNF-α, MCP-1, MIP-1β, and iNOS analyzed by RT-PCR technique representing differential patterns of transcriptional regulation in all the four groups. β-Actin is serving as the house keeping gene. **k** Quantitative analysis of the cDNA bands normalized with β-actin in densitometric units. The values are mean ± SD of three independent experiments with four different animals from each group. $^{a}p \leq 0.05$, $^{b}p \leq 0.01$, and $^{c}p \leq 0.001$ in comparison to control, $^{y}p \leq 0.01$ and $^{z}p \leq 0.001$ in comparison to DMH by one-way ANOVA. **l** qRT-PCR analysis of iNOS mRNA to validate the RT-PCR results showing significantly higher expression of iNOS mRNA in the DMH group as compared to the others. β-Actin served as a reference gene for the normalization of expression profiles in each group. The values are mean ± SD of three independent experiments with four different animals from each group. $^{a}p \leq 0.05$, $^{b}p \leq 0.01$, and $^{c}p \leq 0.001$ in comparison to control, $^{z}p \leq 0.001$ in comparison to DMH by one-way ANOVA. **m** Quantification of NO was done from the standard curve (1.25–10 nmol) and values expressed in nanomoles per milligram protein which shows higher activity of iNOS enzyme in the DMH group as compared to the control. The values are mean ± SD of three independent experiments with four different animals from each group. $^{b}p \leq 0.01$ and $^{c}p \leq 0.001$ in comparison to control, $^{x}p \leq 0.05$, $^{y}p \leq 0.01$ in comparison to DMH by one-way ANOVA. **n** Quantification of L-citrulline with the help of standard curve (1–7 μmol) where the values expressed in micromole per milligram protein and show higher presence of L-citrulline in the DMH group as compared to the others which validates that the production of NO is via L-arginine pathway and mediated by the activated iNOS enzyme. The values are mean ± SD of three independent experiments with four different animals from each group. $^{b}p \leq 0.01$ in comparison to control, $^{x}p \leq 0.05$ in comparison to DMH by one-way ANOVA

revealed large pools of secreted acid or neutral mucopolysaccharides (arrows), higher number of blood capillaries (circles), dysplastic crypts (broken arrows), and incidence of invasiveness (dotted arrows) in DMH group as compared to control giving a clear sign of highly invasive mucinous adenocarcinoma. However, all these carcinogenic changes were observed to be reverted in DMH + Sulindac and DMH + Celecoxib groups with less number of mucin secreting aberrant crypts and blood vessels with no evidence of invasiveness as compared to DMH alone.

Regulation of Inflammation During Carcinogenesis

Significantly higher protein expression of pro-inflammatory cytokines, i.e., IL-1β, IL-2, IFNγ (Fig. 2a, b) were observed in DMH group via western blot analysis. DMH + Sulindac and DMH + Celecoxib groups are having less expression of these pro-inflammatory cytokines as compared to DMH alone. Immunofluorescence of IL-1β (Fig. 2c), IL-2 (Fig. 2d), IFNγ (Fig. 2e) also supports the western blot results representing higher expression and localization (arrows) of these cytokines in DMH alone group as compared to the others. The mRNA expression of IL-1β via RT-PCR (Fig. 2j, k) also supports its role in DMH-induced colon carcinogenesis mediated through inflammation, whereas NSAIDs co-administration has negatively regulated its mRNA expression. Supplementary Fig. 1 shows the putative mechanism behind the negative regulation of inflammatory response via Sulindac and Celecoxib as both of these drugs can easily dock into the IL-1β-binding site of IL-1 receptor type 1 after replacing the antagonist peptide AF10847. The GLIDE scores (−2.49 and −5.67 with respect to Sulindac and Celecoxib, respectively) and the residues involved in the interactions between the drugs and protein are documented in Table 1.

With the co-administration of NSAIDs higher protein expression of two cytokines, i.e., IL-4 and TNF-α was observed as compared to DMH group via western blot analysis (Fig. 2a, b). This was further confirmed by immunofluorescence as both DMH + Sulindac and DMH + Celecoxib groups are having higher expression and localization (arrows) of IL-4 (Fig. 2f) and TNF-α (Fig. 2g) as compared to DMH. Higher expression of TNF-α

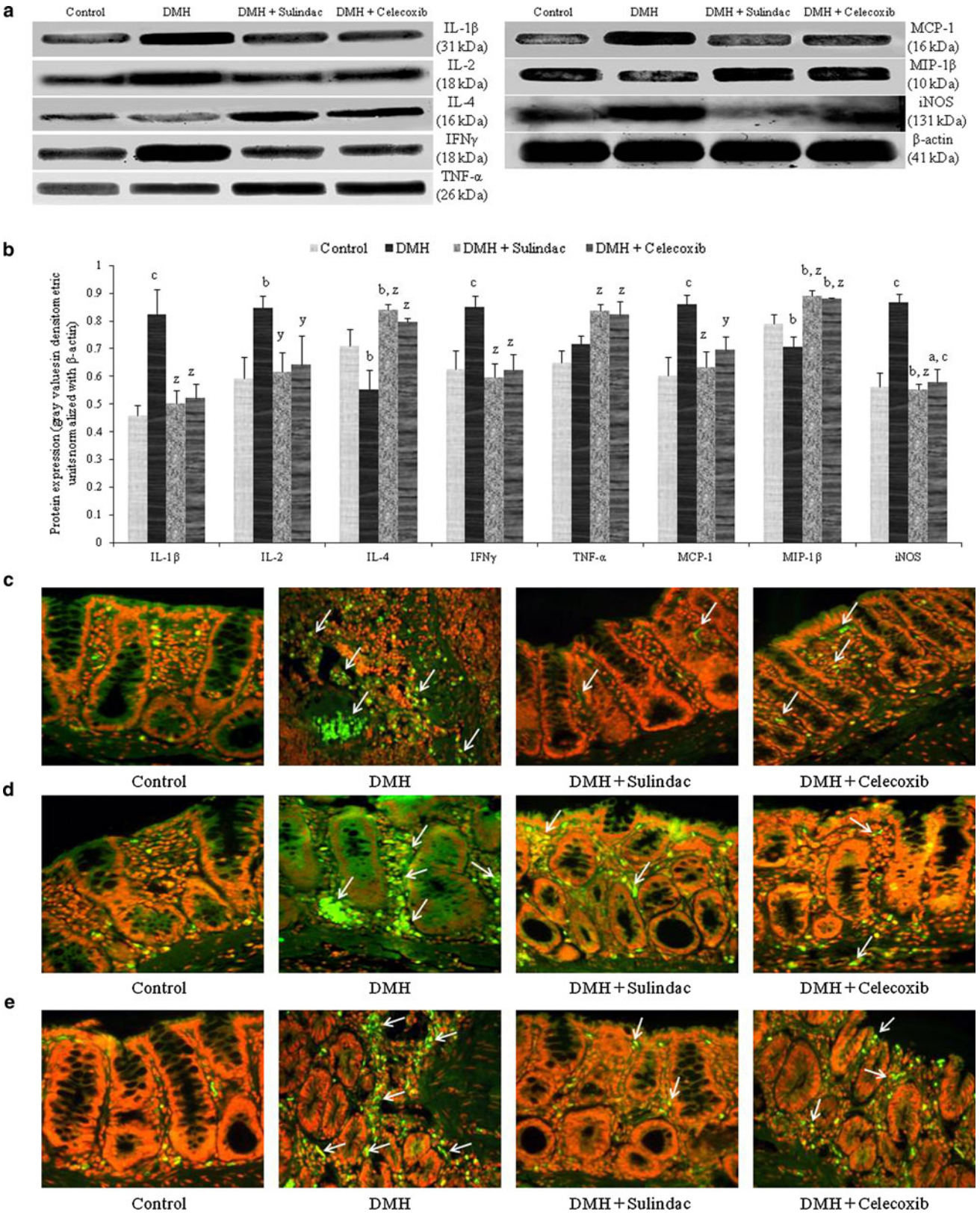
a
Control
DMH
DMH + Sulindac
DMH + Celecoxib
IL-1β (31 kDa)
IL-2 (18 kDa)
IL-4 (16 kDa)
IFNγ (18 kDa)
TNF-α (26 kDa)
MCP-1 (16 kDa)
MIP-1β (10 kDa)
iNOS (131 kDa)
β-actin (41 kDa)
b
Protein expression (gray values in densitometric units normalized with β-actin)
IL-1β
IL-2
IL-4
IFNγ
TNF-α
MCP-1
MIP-1β
iNOS
c
d
e
Control
DMH
DMH + Sulindac
DMH + Celecoxib

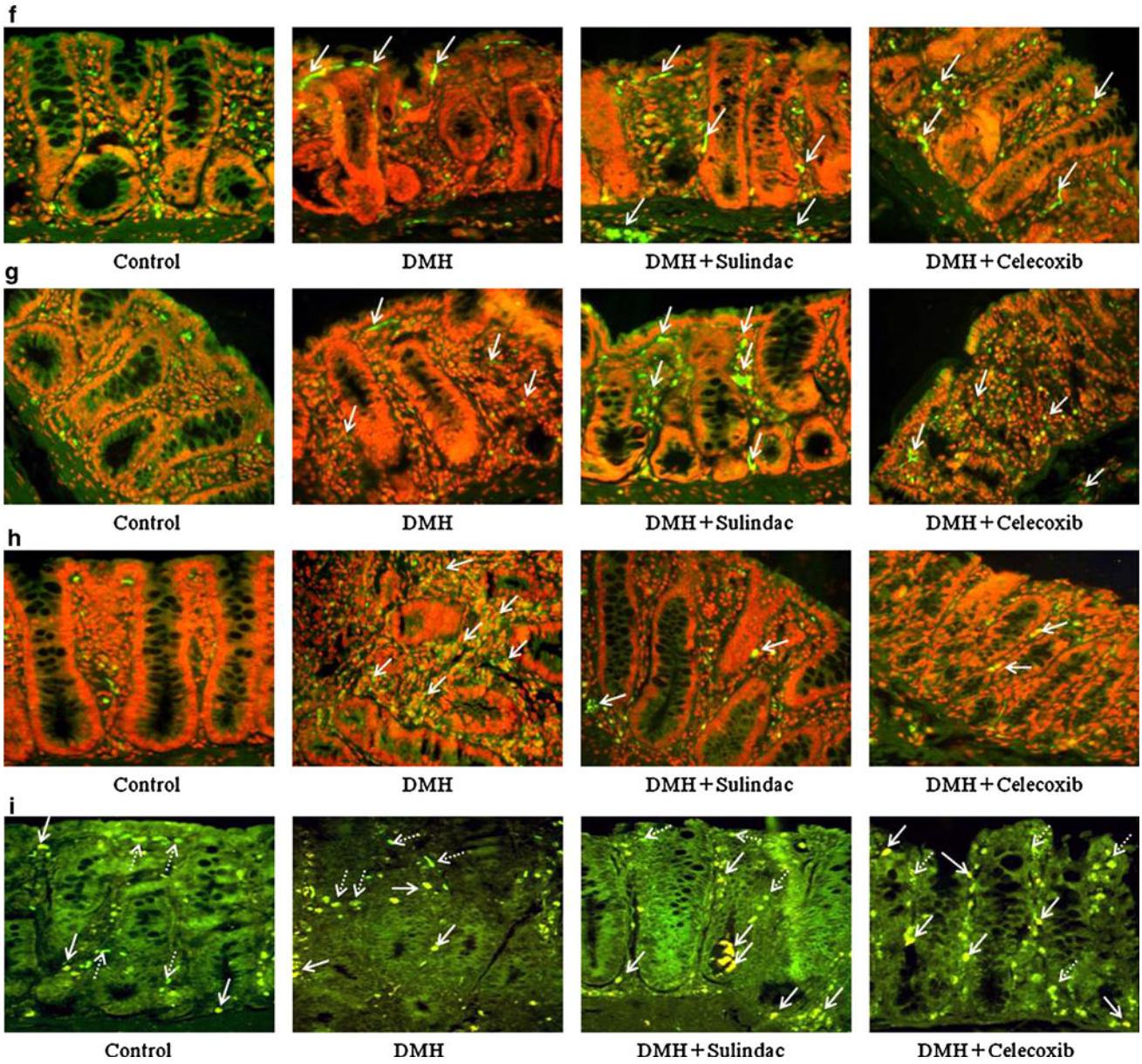

Fig. 2 continued

at mRNA level was also observed in NSAIDs co-administered groups as compared to DMH (Fig. 2j, k). However, DMH alone group shows higher expression of TNF-α both at protein (Fig. 2a, b) and mRNA levels (Fig. 2j, k) as compared to the control group.

MCP-1, a pro-inflammatory chemokine, was observed over-expressed in DMH group both at protein (Fig. 2a, b) and mRNA levels (Fig. 2j, k) as compared to control. However, with NSAIDs co-administration the aberrant expression of MCP-1 was found to be significantly reduced as compared to the DMH alone. NSAIDs co-administration shows a significant increase in the expression of anti-tumor chemokine MIP-1β both at protein (Fig. 2a, b) and mRNA levels (Fig. 2j, k) suggesting the role of Sulindac and Celecoxib in inducing host anti-tumor innate immunity which could be mediated by T cells or dendritic cells or natural killer cells.

Fluorescence co-staining with CD4-FITC and CD8-PE monoclonal antibodies (Fig. 2i) revealed a higher localization of CD8+ cells (cytotoxic T-lymphocytes or natural killer cells or dendritic cells) in NSAIDs co-administered groups (arrows) as compared to the DMH group which, on the other hand, showed higher localization of CD4+ cells (either T-helper cells or monocytes; dotted arrows). These results co-relate with the findings of MCP-1 and MIP-1β expressions in the different groups.

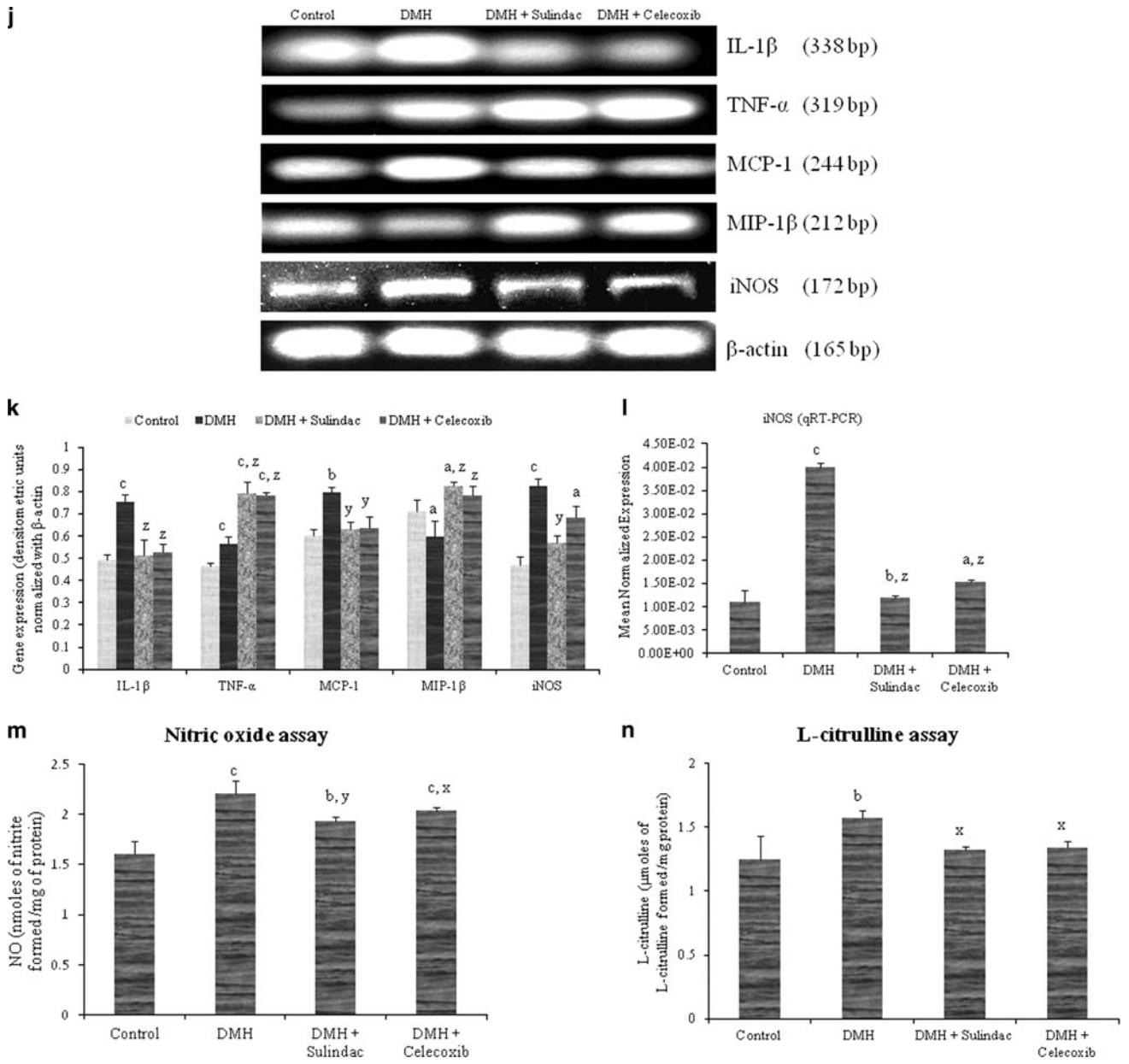

Fig. 2 continued

Association of DMH-induced carcinogenesis with inflammation in colonic tissue was further confirmed with the over-expression of protein (Fig. 2a, b) and mRNA levels (Fig. 2j, k) of the inflammatory marker enzyme iNOS. The mRNA expression of iNOS was further validated by qRT-PCR (Fig. 2l). Higher expression and localization of iNOS in aberrant crypts were also observed by immunofluorescence (Fig. 2h) in the DMH group as compared to the control group. However, NSAIDs co-administration has significantly reduced iNOS in the colonic tissue.

Higher activation of iNOS is linked with the generation of NO which has been observed as a vasodilator and could help in the infiltration of inflammatory cells and thereby promoting neovascularization. NO is generated when L-arginine is metabolized by iNOS enzyme to L-citrulline. We observed an increased production of NO (Fig. 2m) and L-citrulline (Fig. 2n) in DMH group as compared to control. NSAIDs co-administration has significantly reduced the production of both NO and L-citrulline as compared to DMH alone. Our *in silico* experiments also hypothesize a mechanism for the inhibition of iNOS activity by Sulindac and Celecoxib as these NSAIDs were efficiently docked into the nitrosation site of the enzyme which is essential for NO production and release (Supplementary Fig. 2) where the docking reactions were performed by replacing already

Fig. 3 Differential regulation of various transcription factors and their upstream regulatory molecules during carcinogenesis. **a** Western blot analysis of the pro-inflammatory and cell survival transcription factors, i.e., Stat3 and NF-κB suggesting their essential role in the DMH-induced colon carcinogenesis as both of these proteins along with their upstream regulators Jak3 and IKK (subunit IKKβ), respectively, were found significantly overexpressed in the DMH group in comparison to the vehicle-treated control group. However, with NSAIDs co-administration the negative regulator of NF-κB activation, i.e., IκB protein (subunit IκBβ) which sequesters NF-κB into the cytoplasm and restricts its release to localize in nucleus for transcription of various pro-inflammatory and cell survival molecules, was found to be upregulated in DMH + Sulindac and DMH + Celecoxib groups as compared to the DMH alone. NSAIDs co-administration also downregulated the expression profiles of Jak3 and Stat3 proteins as compared to the DMH. Another anti-inflammatory and NF-κB antagonistic transcription factor, i.e., PPARγ was observed significantly upregulated in DMH + Sulindac and DMH + Celecoxib groups as compared to the DMH alone. **b** Quantitative analysis of the blots normalized with β-actin in densitometric units. The values are mean ± SD of three independent experiments with four different animals from each group. $^{a}p \leq 0.05$, $^{c}p \leq 0.001$ in comparison to control, $^{x}p \leq 0.01$, $^{y}p \leq 0.01$, and $^{z}p \leq 0.001$ in comparison to DMH by one-way ANOVA. **c** Immunofluorescence analysis (×400) of NF-κB protein showing higher expression (*dotted arrows*) and increased nuclear localization (*arrows*) of this transcription factor in the DMH-treated groups, whereas DMH + Sulindac and ▶ DMH + Celecoxib groups show significantly lower expression (*dotted arrows*) and thereby lower nuclear localization of NF-κB as compared to the DMH group. **d** Immunofluorescence analysis (×400) of anti-inflammatory transcription factor, i.e., PPARγ representing its higher expression (*dotted arrows*) and increased nuclear localization (*arrows*) in DMH + Sulindac and DMH + Celecoxib groups as compared to the DMH alone. **e** mRNA expression analysis of IKKβ, IκBβ, NF-κB, and PPARγ via RT-PCR also supports the western blot and immunofluorescence results for the respective genes. The mRNA expression profile of IKKβ and NF-κB was found significantly upregulated in the DMH group, whereas mRNA levels of IκBβ and PPARγ were found to be significantly upregulated in DMH + Sulindac and DMH + Celecoxib groups. β-Actin is serving as the house keeping gene. **f** Quantitative analysis of the cDNA bands normalized with β-actin in densitometric units. The values are mean ± SD of three independent experiments with four different animals from each group. $^{a}p \leq 0.05$, $^{b}p \leq 0.01$, and $^{c}p \leq 0.001$ in comparison to control, $^{y}p \leq 0.01$ and $^{z}p \leq 0.001$ in comparison to DMH by one-way ANOVA. **g** qRT-PCR results also validated the RT-PCR observations in (**f**). β-Actin served as a reference gene for the normalization of expressions in each group. The values are mean ± SD of three independent experiments with four different animals from each group. $^{a}p \leq 0.05$, $^{b}p \leq 0.01$, and $^{c}p \leq 0.001$ in comparison to control, $^{y}p \leq 0.01$ and $^{z}p \leq 0.001$ in comparison to DMH by one-way ANOVA

Table 1 Molecular docking study revealing the interaction between various proteins and their putative amino acids of the binding site with the ligands (viz. Sulindac and Celecoxib) via hydrogen bonds (H-bonds) formation

Ligands	Proteins	Amino acids involved in H-bond formation	Length of the H-bond (Å)	GLIDE scores
Sulindac	Interleukin-1 receptor type 1 (PDB ID: 1G0Y)	Glu 129: (H)	2.350	−2.49
Celecoxib		Gln 113: (O)	2.513	−5.67
		Leu 115: (O)	2.383	
		Val 124: (O)	2.573	
		Val 124: (O)	1.709	
Sulindac	Inducible nitric oxide synthase (PDB ID: 3NQS)	Thr 370: (H)	1.744	−3.55
Celecoxib		Trp 457: (O)	1.822	−8.45
Sulindac	Jak3 (PDB ID: 1YVJ)	Asp967: (H)	1.693	−9.46
Celecoxib		Arg 953: (H)	2.340	−9.77
		Arg 953: (H)	1.813	
		Asn 954: (O)	1.667	
		Asp 967: (O)	1.893	
		Gln 988: (H)	2.470	
Sulindac	Stat3 (PBD ID: 1BG1)	Gln 635: (H)	1.911	−4.08
Celecoxib		Gln 635: (H)	1.600	−4.41
		Ser 636: (O)	1.711	
		Ser 636: (H)	2.469	
Sulindac	VEGFR1 (PDB ID: 3HNG)	Arg 1021: (H)	2.584	−5.16
		Arg 1021: (H)	1.925	
Celecoxib		Asp 1040: (O)	2.376	−5.17
Sulindac	VGEFR2 (PDB ID:1Y6A)	Cys 917: (H)	1.794	−5.47
Celecoxib		Lys 866: (H)	1.984	−5.48
		Phe 1045: (O)	1.774	

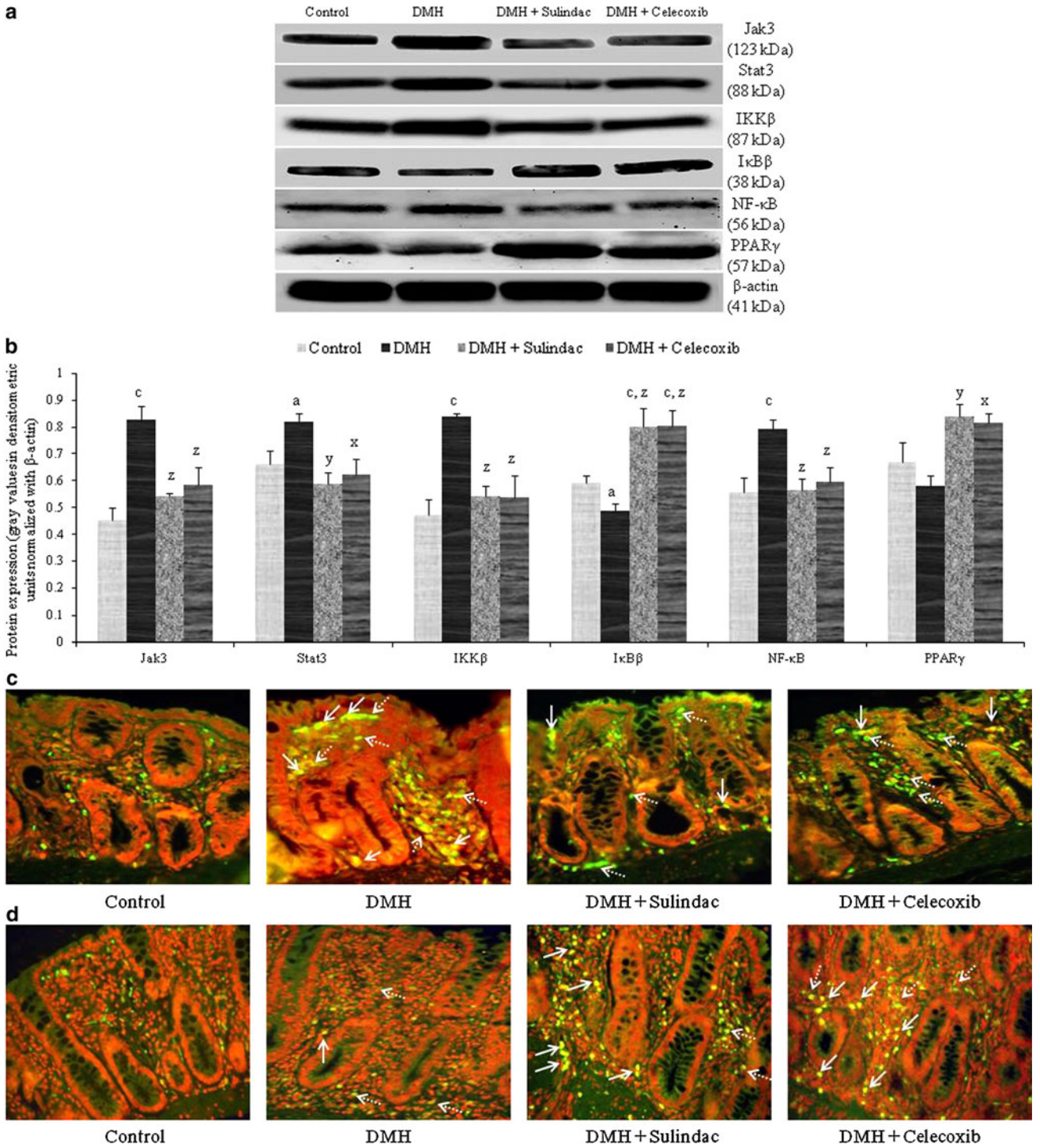

bound NOS inhibitor ethyl 4-[(4-methylpyridin-2-yl)amino]piperidine-1-carboxylate by Sulindac and Celecoxib. Sulindac and Celecoxib achieved favorable GLIDE scores (−3.55 and −8.45, respectively) for their docking stability and were also observed to interact with the active site residues via forming H-bonds (Table 1).

Role of Transcription Factors During Carcinogenesis

Jak3, a cell survival kinase, was observed over-expressed in DMH group as compared to the control by western blot analysis (Fig. 3a, b). Stat3 which is a downstream target for activated Jak3 and functions as a transcription factor

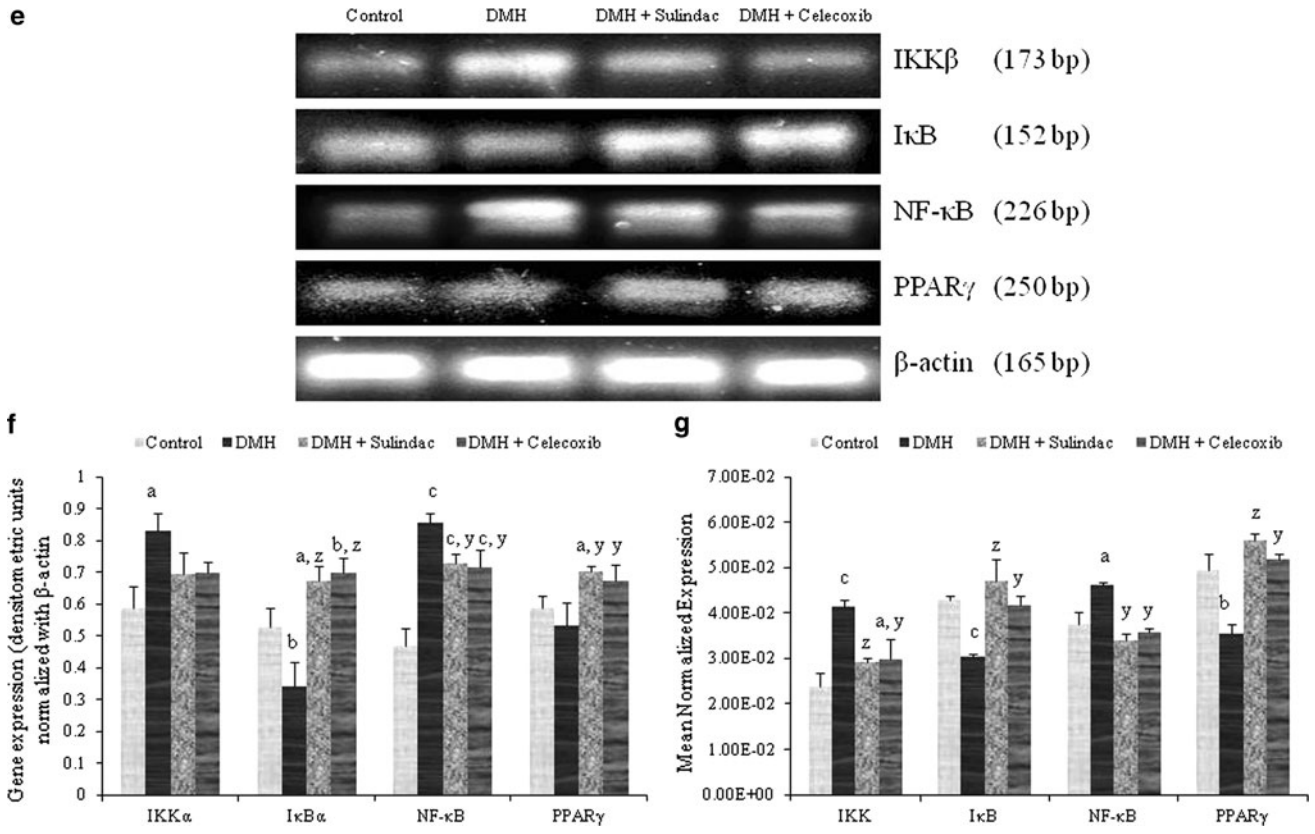

Fig. 3 continued

for various pro-inflammatory cytokines, growth factors, and anti-apoptotic agents, was also observed abruptly elevated in the nuclear fractions of DMH group as compared to control (Fig. 3a, b). However, with NSAIDs co-administration protein expression levels of Jak3 and nuclear translocation of Stat3 were significantly reduced as compared to the DMH alone group. Our *in silico* docking experiments also strongly suggest an inhibition of Jak3 activation by these NSAIDs as they docked into the ATP-binding pocket or catalytic site of Jak3 (Supplementary Fig. 3) with favorable GLIDE scores (−9.46 and −9.77 with respect to Sulindac and Celecoxib, respectively; Table 1). Sulindac (Glide score = −4.08) and Celecoxib (Glide score = −4.41) could also attenuate Stat3 molecule's DNA binding as well as transcriptional activity because these drugs were observed to be efficiently docked into the SH2 domain of Stat3 (Supplementary Fig. 4; Table 1) responsible for Stat3 dimerization and activation.

In response to the pro-inflammatory cytokines' intracellular downstream signaling, erratically elevated nuclear localization of pro-inflammatory and cell survival transcription factor NF-κB was also observed significantly in DMH group as compared to the control by western blot analysis (Fig. 3a, b) which was further validated by immunofluorescence (Fig. 3c) where DMH group showed higher incidence of nuclear localization (yellow fluorescence due to FITC and PI together) of NF-κB (arrows) and also cytoplasmic incidence (green fluorescence due to FITC alone represented by dotted arrows) as compared to the other groups. DMH animals were also found to have significantly elevated levels of NF-κB mRNA (cytoplasmic expression) as checked via RT-PCR (Fig. 3e, f) and further validated by qRT-PCR (Fig. 3g). The upstream kinase for NF-κB activation, i.e., inhibitory protein-B kinase or IKK (subunit IKKβ) which regulates its nuclear localization via the phosphorylation of the bound IκB was found over-expressed both at protein (Fig. 3a, b) and mRNA levels (Fig. 3e–g) in DMH group as compared to control suggesting that activation of NF-κB during carcinogenesis could be mediated through the IKK downstream signaling. With the co-administration of Sulindac and Celecoxib, a significant decrease in NF-κB nuclear localization (Fig. 3a–c) and mRNA levels (Fig. 3e–g) were observed as compared to DMH alone. This negative regulation of NF-κB during NSAIDs co-administration could be mediated through the downregulation of IKK, but the upregulation of IκB (subunit IκBβ; which sequesters NF-κB in the

cytoplasm and prevents its translocation into nucleus) both at protein (Fig. 3a, b) and mRNA levels (Fig. 3e–g).

NSAIDs co-administration not only negatively regulated the pro-inflammatory transcription factors but also upregulated nuclear localizations of the anti-inflammatory transcription factor, i.e., PPARγ. Higher levels of nuclear localized PPARγ were observed in DMH + Sulindac and DMH + Celecoxib groups in comparison to DMH alone as analyzed via western blot (Fig. 3a, b) and further validated by immunofluorescence (Fig. 3d) as arrows show the nuclear localized PPARγ and dotted arrows show the cytoplasmic PPARγ (yellow and green fluorescence, respectively). Along with the protein expression, mRNA levels of PPARγ were also observed higher in NSAIDs co-administered groups in comparison to DMH alone as analyzed by RT-PCR (Fig. 3e, f) and further validated by qRT-PCR analysis (Fig. 3g).

Regulation of Angiogenic Factors During Carcinogenesis

Activation of NF-κB during carcinogenesis in DMH group has also positively regulated the expression of pro-inflammatory cox-2 gene as observed by RT-PCR (Fig. 4a, b) and further validated by qRT-PCR analysis (Fig. 4c). However, Celecoxib which is a selective COX-2 inhibitor has significantly downregulated cox-2 gene expression as compared to Sulindac (COX non-specific) and DMH treatment. There were no significant variations in the mRNA expression patterns of the housekeeping gene cox-1 among all the groups as expected (Fig. 4a–c). Western blot analysis showed an over-expression of COX-2 in DMH group as compared to control (Fig. 4d, e). Higher expression of COX-2 in colonic tissue section of DMH group as compared to the other groups was also observed by immunofluorescence (Fig. 4f). However, COX-2 protein levels as well as tissue localizations were found down-regulated with the co-administration of NSAIDs in comparison to DMH alone. Celecoxib showed a significant decrease in COX-2 protein expression and localization as compared to Sulindac which co-relates with the mRNA analysis. Alike to mRNA levels no significant change in COX-1 protein expression was observed among all the treatment groups (Fig. 4d, e).

Higher expression of COX-2 enzyme in DMH group could be responsible for the generation of increased concentrations of PGE_2 via arachidonic acid metabolism (Fig. 4h) which might possibly help in vasodilation and neovascularization. However, alike COX-2 expression, NSAIDs co-administration has significantly downregulated the production of PGE_2 as compared to DMH alone.

Aberrant upregulation of angiogenic factor, VEGF-A, was observed at mRNA level in DMH group as compared to control by RT-PCR (Fig. 4a, b) and further validated by qRT-PCR (Fig. 4c) whereas NSAIDs co-administration has significantly reduced that. Alike the mRNA levels, the protein expression of VEGF-A was also significantly higher in DMH alone as compared to the control (Fig. 4d, e) and NSAIDs co-administration has negatively regulated the same. Immunofluorescence analysis validated the western blot results showing higher localization of VEGF-A inside the colonic tissue of DMH in comparison to other groups (Fig. 4g). We observed that a putative angiostatic mechanism could be followed by Sulindac and Celecoxib via *in silico* docking studies and that these drugs efficiently docked in the VEGF-A-binding site of VEGF-A receptors, i.e., VEGFR1 (Supplementary Fig. 5) and VEGFR2 (Supplementary Fig. 6) with favorable GLIDE scores (Table 1).

For the initiation of angiogenesis breakdown of extracellular matrix is necessary to promote the generation of new blood capillaries inside the neoplasm which could possibly be mediated by various matrix metalloproteinases such as MMP-2 (gelatinase A) and MMP-9 (gelatinase B). We observed a significantly upregulated mRNA expression of MMP-2 and MMP-9 in DMH group as compared to the control by RT-PCR (Fig. 4a, b) and further validated by qRT-PCR (Fig. 4c), whereas DMH + Sulindac and DMH + Celecoxib groups show a significant reduction of mRNA levels as compared to DMH alone. The protein expression levels of MMP-2 and MMP-9 also co-related with the higher mRNA expression as observed in DMH group compared to the control (Fig. 4d, e). However, with the co-administration of NSAIDs a significant decrease in MMP-2 and MMP-9 protein expression was observed as compared to DMH alone. The relative activities of MMP-2 and MMP-9 in different groups were determined by gelatin zymography where these proteins were differentiated according to their molecular weights of respective pro- or inactivated and activated forms and gelatin degradation activity. In DMH-treated group, an increased quantity of active MMP-2 (mol. wt. ~67 kDa) and MMP-9 (mol. wt. ~84 kDa) was observed as compared to control, whereas NSAIDs co-administered groups have lesser amounts of both pro- and active MMP-2 and MMP-9 (Fig. 4i). This suggests that the activated MMPs play a significant role in tumor angiogenesis and NSAIDs may check it via inhibition of MMPs.

Regulation of Apoptosis During Carcinogenesis

Imbalance between proliferation and apoptosis has been observed as a possible mechanism for carcinogenesis but the role of this imbalance during inflammatory colorectal cancer is still unclear. With flowcytometric analysis (Fig. 5a, b) we observed that due to inflammation, not only the number of apoptotic cells was decreased in DMH group

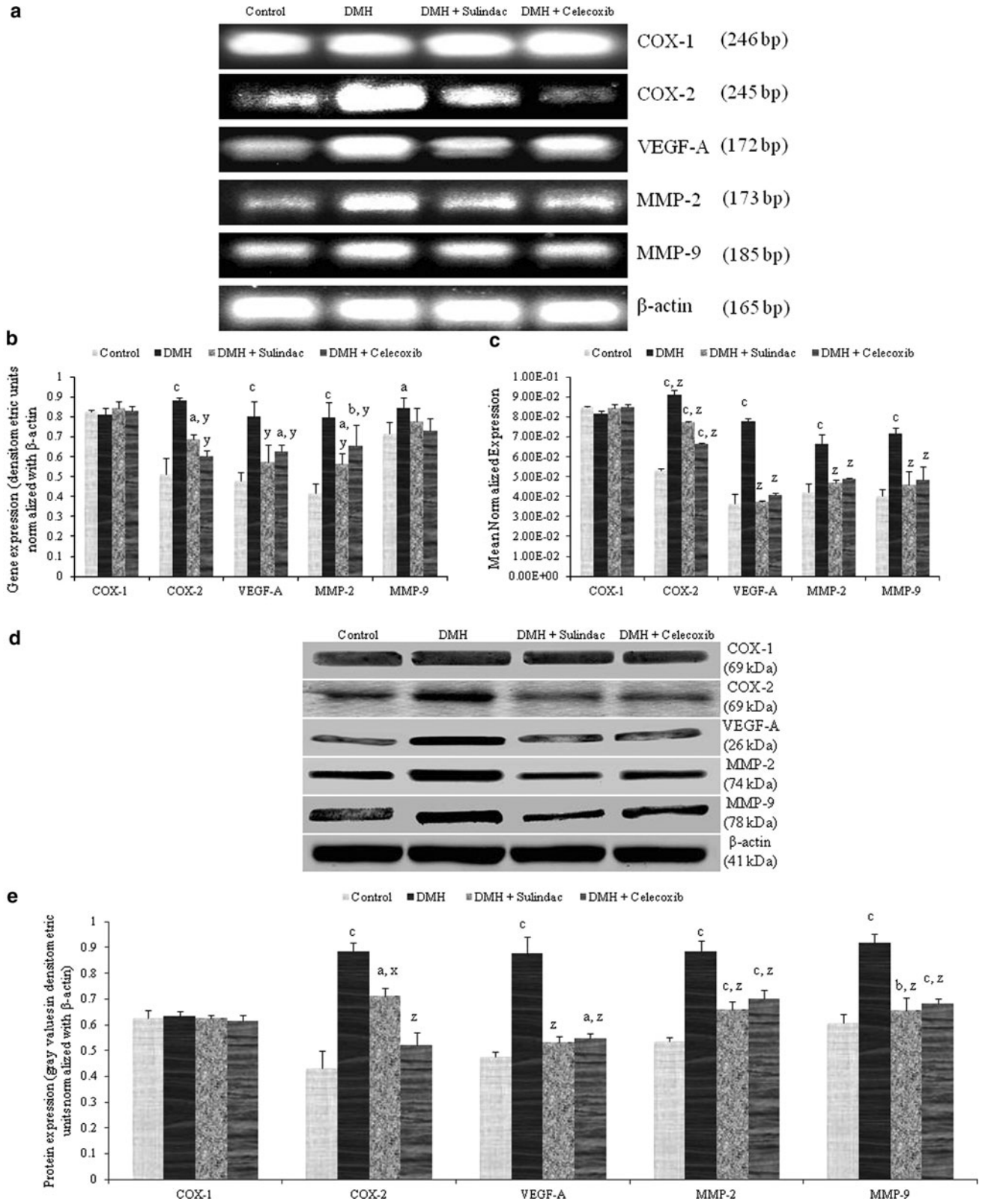

(Annexin-V +ve cells in lower right quadrant) but also the survival of colonocytes was also increased (lower left quadrant) as compared to the control where a basal apoptotic rate is maintained. However, NSAIDs co-administration has induced apoptosis in colonocytes with more number of cells in early phase of apoptosis (Annexin

Fig. 4 Role of various pro-angiogenic factors during inflammatory colorectal cancer. **a** Post-transcriptional (mRNA) analysis of various genes using RT-PCR revealed that COX-2, VEGF-A, MMP-2, and MMP-9 were significantly upregulated during carcinogenesis in the DMH groups as compared to the control, whereas NSAIDs co-administration has significantly reduced their expressions as compared to the DMH alone. COX-1 which is a homeostatic housekeeping gene was observed with no significant difference among all the four groups. β-Actin is serving as the house keeping gene. **b** Quantitative analysis of the cDNA bands normalized with β-actin in densitometric units. The values are mean ± SD of three independent experiments with four different animals from each group. $^{a}p \leq 0.05$, $^{b}p \leq 0.01$, and $^{c}p \leq 0.001$ in comparison to control, $^{y}p \leq 0.01$ in comparison to DMH by one-way ANOVA. **c** qRT-PCR analysis of pro-angiogenic factors also validated the results of RT-PCR where these were found significantly elevated in DMH group as compared to the others which suggests the continuing occurrence of angiogenesis during carcinogenesis. Lower gene expression of these pro-angiogenic factors in DMH + Sulindac and DMH + Celecoxib groups points toward the possible angiostatic role of these NSAIDs in colorectal cancer. Expression of COX-1 was again observed with no significant change among all the four groups. β-Actin served as a reference gene for the normalization of expressions in each group. The values are mean ± SD of three independent experiments with four different animals from each group. $^{c}p \leq 0.001$ in comparison to control, $^{z}p \leq 0.001$ in comparison to DMH by one-way ANOVA. **d** Western blot analysis of pro-angiogenic factors, i.e., COX-2, VEGF-A, MMP-2, and MMP-9 represents their significant upregulation during DMH-induced colon carcinogenesis, whereas being a homeostatic housekeeping protein COX-1 was found with no significant change among all the four groups. β-Actin is serving as loading control. **e** Quantitative analysis of the blots normalized with β-actin in densitometric units. The values are mean ± SD of three independent experiments with four different animals from each group. $^{a}p \leq 0.05$, $^{b}p \leq 0.01$, and $^{c}p \leq 0.001$ in comparison to control, $^{x}p \leq 0.05$, $^{z}p \leq 0.001$ in comparison to DMH by one-way ANOVA. **f** Immunofluorescence analysis (×400) of COX-2 protein showing its higher expression (*arrows*) in the DMH-treated group as compared to the control. However, NSAIDs co-administered groups have lower expression and localization of COX-2 as compared to the DMH. **g** Immunofluorescence analysis (×400) of VEGF-A protein representing its higher expression (*arrows*) in the DMH in comparison to the control, whereas NSAIDs co-administration seems to have downregulated the expression of VEGF-A. **h** Quantification of PGE_2 was done from the standard curve (39.1–2,500 pg/ml) and values were expressed in picograms per milliliter protein which shows higher activity of COX-2 enzyme in the DMH group as compared to the control. The values are mean ± SD of three independent experiments with four different animals from each group. $^{b}p \leq 0.01$ in comparison to control, $^{x}p \leq 0.05$ and $^{y}p \leq 0.01$ in comparison to DMH by one-way ANOVA. **i** Gelatin zymography to analyze the differential activity of the matrix metalloproteinases where DMH group is having higher presence of activated MMP-2 and MMP-9 with respect to their "pro" forms (zymogens) suggesting their role in the degradation of extra cellular matrix (ECM) during angiogenesis. DMH + Sulindac and DMH + Celecoxib groups are showing less activated as well as pro forms of MMP-2 and MMP-9, respectively

V-FITC +ve cells in lower right quadrant) and also in executioner phase of apoptosis (both Annexin V-FITC and 7-AAD +ve cells in upper right quadrant). This assay co-relates with the results that being anti-inflammatory in action these NSAIDs can also induce apoptosis in colonocytes by upregulating the anti-inflammatory cytokines like IL-4 and TNF-α.

Discussion

In 1983, Rudolf Virchow was the first person to propose the role of inflammation in carcinogenesis as he observed the presence of leukocyte infiltration in neoplastic tissues [25]. We have earlier observed the role of inflammation in the early phase of experimental colorectal cancer and chemopreventive role of NSAIDs (viz. Sulindac and Celecoxib) [14]. In this study, we demonstrate the persistency of inflammation and induction of angiogenesis during the advanced phase of colorectal carcinogenesis and that various ways of chemoprevention could be followed by two NSAIDs, viz., COX non-specific, Sulindac and COX-2 specific, Celecoxib.

The morphological examinations of dissected colons from different animal groups showed up with full-grown tumors along with the clear signs of aberrant blood supply network in DMH group as compared to control whereas NSAIDs co-administered groups have significantly reduced the number and size of these tumors. Histopathological studies also represented higher invasion, more number of blood capillaries, aberrant dysplastic crypts, and pools of secreted acidic/neutral mucopolysaccharides collectively suggesting the incidence of highly invasive mucinous adenocarcinoma in DMH group whereas with the NSAIDs co-administration tissue architecture is better and showing less aberrant features as compared to DMH.

Higher expression of pro-inflammatory cytokine IL-1β has been reported in various malignancies, e.g., lung cancer, pancreatic carcinoma, etc., and also the genetically ablated IL-1β carrying mice showed an absence of metastatic tumors suggesting its importance in propagation of inflammation and thereby carcinogenesis [1, 9]. We observed a higher expression of IL-1β both at mRNA and protein levels also supported by higher localization in neoplastic tissue of DMH-treated animals as compared to the control animals. However, NSAIDs co-administration has significantly reduced its expression. The negative regulation of IL-1β and thereby decrease in inflammation could be mediated via a novel putative IL-1β receptor type 1 blocking mechanism [26] by Sulindac and Celecoxib and it could be stated that NSAIDs binding to the IL-1β receptor might create a negative feedback response for IL-1β expression.

Cytokines exhibit pleiotropic nature as they could regulate the expression of various other cytokines, e.g., induction of IL-1β could apparently induce IL-2 expression via increased IL-2R expression and thereby helps in maintaining an inflammatory state [27]. However,

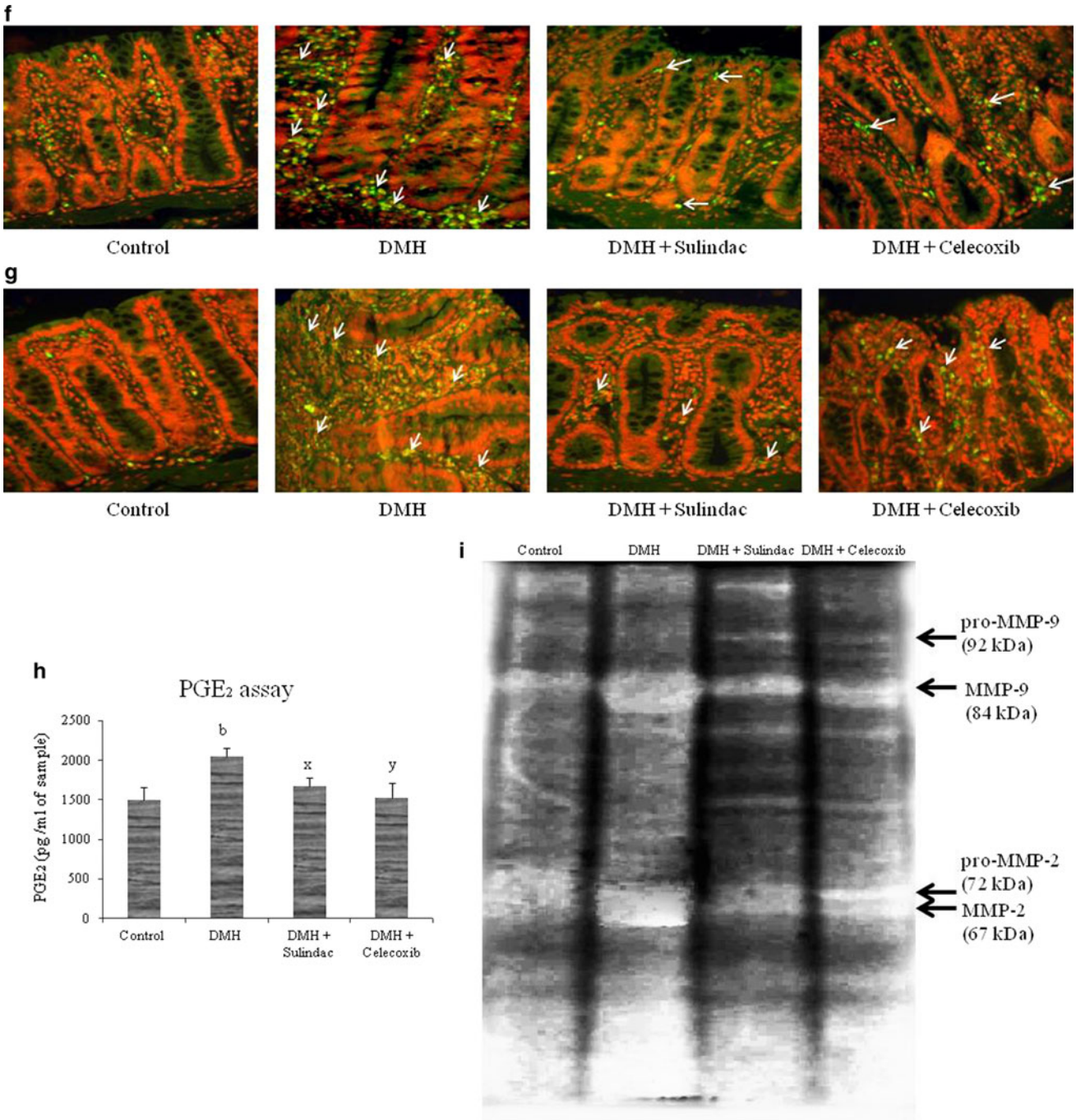

Fig. 4 continued

increased expression of anti-inflammatory cytokine, IL-4 has been reported to downregulate IL-2 expression via the induction of PPARγ which is a ligand-dependent transcription factor and has been previously reported as anti-inflammatory in nature [28, 29]. Our study also supports this hypothesis as we observed a higher expression of IL-2 in DMH-treated group, whereas IL-4 and PPARγ expression levels were higher in NSAIDs co-administered groups. Moreover, Sulindac has also been reported as an activator of PPARγ and could also serve as its ligand [11]. Higher nuclear localization of PPARγ in NSAIDs co-administered groups strengthens its role as an anti-inflammatory and thereby anti-neoplastic biomolecule.

IL-2 is an important factor for the stimulation of helper T-lymphocytes (CD4+ T-cells) and could induce cell death (AICD) in activated cytotoxic T-lymphocytes (CD8+ T-cells) thereby preventing the cancer cells to be recognized as non-self and helping in tumor progression

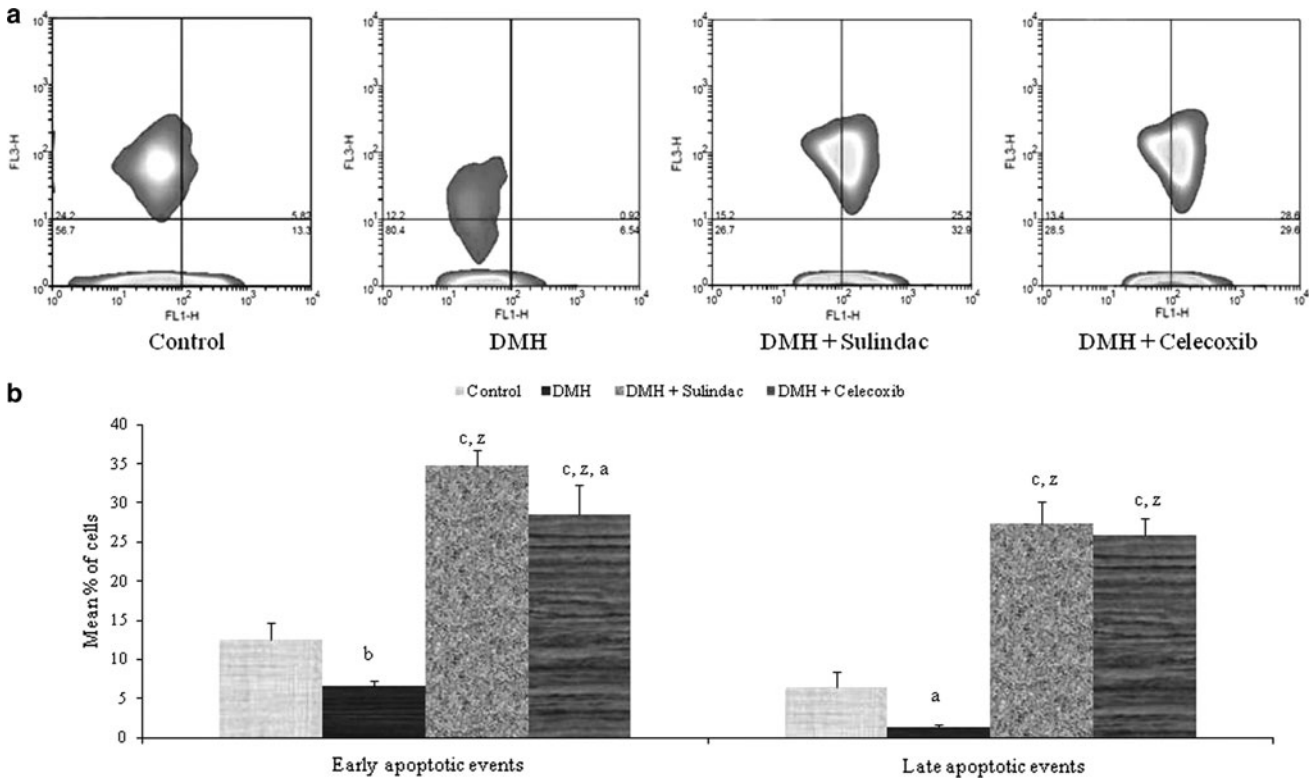

Fig. 5 Analysis of apoptotic potential by Annexin V-FITC/7-AAD co-staining of the isolated colonocytes. **a** Contour plots showing the distribution of colonocytes according to early apoptotic (*lower right quadrant*), late apoptotic (*upper right quadrant*), necrotic or dead cells (*upper left quadrant*), and live or unstained cells (*lower left quadrant*). Markers were set according to all compensation controls with blank corrections. DMH + Sulindac and DMH + Celecoxib are showing higher incidence of early as well as late apoptotic events as compared to the DMH. **b** Graph represents the mean percentage of cells (out of 2×10^4 events) with early or late phase of apoptosis. The values are mean ± SD of three independent experiments with four different animals from each group. $^{a}p \leq 0.05$ and $^{c}p \leq 0.001$ in comparison to control, $^{z}p \leq 0.05$ in comparison to DMH by one-way ANOVA

[8]. We identified that in DMH-induced tumor samples, CD4+ T-cell population was higher as compared to CD8+ T-cells along with the upregulation of IL-2, whereas NSAIDs co-administration has negatively regulated the expression of IL-2 which could be via the above said factors (IL-4 and PPARγ) and has increased the CD8+ T-cells counts to help recognize the cancer cells as non-self and their removal via phagocytosis or other immunologic processes.

IL-2 and IFNγ have been previously observed to promote cell survival and enhanced production of pro-inflammatory factors via activating Jak/Stat pathway in various cancers. Activation of Jak3 via auto-phosphorylation in turn activates Stat3 which leads to its nuclear localization and thereby induces the expression of various cell survival agents [30–35]. We observed aberrant upregulation of Jak3 and Stat3 proteins expressions during carcinogenesis in DMH-treated animals which was found to be significantly downregulated in NSAIDs co-administered groups, and thus propose a putative "two-sword" mechanism for the downregulation of Jak3/Stat3 activation pathway via the interactions of both Sulindac and Celecoxib with these proteins. Both Sulindac and Celecoxib were identified to be efficiently docked into the catalytic site or ATP-binding site responsible for the auto-phosphorylation as well as activation of Jak3 molecule and also interacted with the key residue molecule Asp967 via H-bond [36] suggesting a possible insight of developing new modified drug molecules with better therapeutic intervention. These two drugs were also found to be easily docked into the SH2 domain of Stat3 protein which is responsible for the dimerization of Stat3 molecules and thereby its activation. For the activation of Stat3, two Stat3 monomers dimerize in a reciprocal binding pattern on SH2 domain of one monomer to the Pro-pTyr-Leu-Lys-Thr-Lys sequence of the other monomer [37]. This could be stated here that Sulindac and Celecoxib could prevent inflammation and aberrant cell proliferation as a part of cancer chemoprevention via negatively regulating the Jak3/Stat3 activation pathway.

TNF-α has earlier been reported to function both as tumor promoter molecule if expressed in suitable concentrations but could turn into a tumor suppressor and if present in elevated concentrations [1, 38]. The overall

signaling of TNF-α is regulated via the activation of NF-κB which itself serves as a transcription factor for more than 200 cell survival and oncogenic proteins. It has also been observed that when NF-κB activation was blocked, the elevated TNF-α functioned as anti-tumor cytokine and helped in inducing apoptosis among the cells [39–42]. This study supports the role of Sulindac in blocking NF-κB nuclear translocation as described earlier and also proposes Celecoxib as an inhibitor of NF-κB signaling. With the suppression of NF-κB activation in NSAIDs co-administered groups, the elevated levels of TNF-α served as tumor suppressor and higher incidences of apoptotic events were observed after Annexin V-FITC/PI co-staining. Inactivation of NF-κB in NSAIDs co-administered groups could also be achieved via the higher activation of PPARγ as described in our previous study [13] and has also been observed in various other studies [43, 44].

Along with the downstream signaling of pro-inflammatory cytokine IL-1β via the activation of NF-κB, the prominent marker enzyme for localized inflammation, i.e., iNOS was also observed having elevated levels in DMH group both at mRNA and protein expressions as compared to the others. Higher expression of iNOS is related with the production of a very stable vasodilator molecule, i.e., NO which helps in the infiltration of neutrophils at the site of inflammation [14, 45–48]. We observed that along with its expression, iNOS was very much in its active form to produce NO via L-arginine pathway as L-citrulline levels were high in DMH treatment group. However, NSAIDs co-administration has reduced the expressions (mRNA and protein) as well as the activation of iNOS enzyme to overcome the localized inflammation as both of these NSAIDs were efficiently docked into the nitrosation site of iNOS enzyme which is critical for NO production and release [49]. Therefore, Sulindac and Celecoxib could be efficient inhibitory molecules of the chronic inflammatory state in tumorigenesis, in particular, preventing the iNOS for NO buildup with subsequent DNA damage leading to a domino-type effect, and thereby suppressing neoplastic progression.

Downstream signaling of NF-κB not only regulates the gene expression of various pro-inflammatory factors but also positively regulates the transcription of chemokines which play an important role in sustaining the chronic inflammatory response via attracting more and more neutrophils at the lesion site. We observed that MCP-1, which has earlier been observed to be associated with the increased rate of metastasis and poor prognosis of various cancers [50], was highly expressed (mRNA and protein levels) in DMH group as compared to the others. However, NSAIDs co-administration has not only downregulated MCP-1 expressions but also enhanced the expressions of MIP-1β chemokine (anti-inflammatory) which helps in the recruitment of CD8+ T-cells, natural killer cells (NK cells), and the naïve dendritic cells at the site of inflammation [51]. Recruitment of naïve dendritic cells may lead to the killing of growing cancer cells (having unrecognized cell surface markers and treated as non-self) via innate anti-tumor T-cell response (initiated via CD8+ T-cells). This supports the observations of finding more CD8+ T-cells in the colonic mucosa of the NSAIDs co-administered groups by fluorescence co-staining.

Another important inflammatory marker enzyme COX-2 was found to be over-expressed in DMH group both at mRNA and protein levels as compared to the others which could obviously be regulated in a positive manner by the higher expression of IL-1β and aberrant nuclear localization of NF-κB. Along with higher expression, COX-2 was also found to be aberrantly activated as an increased production of PGE_2 molecule was observed in DMH group, whereas Celecoxib (COX-2 specific) co-administration has significantly reduced the expression and thereby activation of COX-2 enzyme and Sulindac (COX non-specific) co-administration might have negatively regulated COX-2 enzyme activity via an independent PPARγ-mediated pathway [11]. The homeostatic or housekeeping isoform of COX, i.e., COX-1 was detected in the colonic tissues with no significant changes at mRNA as well as protein levels in all the groups.

Two parallel mechanisms (IL-1β downstream signaling via NF-κB activation but independent of COX-2 and COX-2 downstream signaling via PGE_2 and HIF-1α) have been described earlier [1, 5–7] for the activation of angiogenesis via the higher expression of key molecule like VEGF-A in various cancers [52]. We observed an obvious collaborative effect of IL-1β, NF-κB, and COX-2 in significantly enhancing the expression of VEGF-A in the DMH-treated group as compared to the others. However, NSAIDs co-administration has negatively regulated the expression of VEGF-A via downregulating the upstream processes. We suggest a novel putative mechanism that could be followed by Sulindac and Celecoxib to block VEGF-A downstream signaling and thereby create a negative feedback loop for its reduced expression as both of these drugs were observed to block the VEGF-A-binding sites in both of its extracellular receptors VEGFR1 and VEGFR2 [53] via *in silico* molecular docking studies.

VEGF-A is not the only molecule responsible for angiogenesis but there are several others such as matrix metalloproteinases which are required to break the extracellular matrix for the invasion of cells by releasing the membrane bound VEGF molecule [54, 55] which further helps in the release of membrane bound NO to dilate the vessels and attract more endothelial cells (ECs) for blood capillary formation [47, 48]. We observed that MMP-2 (gelatinase A) and MMP-9 (gelatinase B) were significantly higher in DMH group both at transcriptional and at

translational levels as compared to the other groups. Along with higher expression, an increased level of activated MMP-2 and MMP-9 was also observed via gelatin zymography in DMH group. NSAIDs co-administration has reduced the expression levels as well as the activated forms of these MMPs as compared to DMH alone suggesting that Sulindac and Celecoxib could also function as anti-angiogenic molecules also, besides being pro-apoptotic [11–14].

Conclusion

This study describes the role of chronic inflammation in angiogenesis during the advanced stage of chemically induced colorectal cancer. Various factors function synergistically or antagonistically to regress malignancy and angiogenesis and thereby improve the chance of targeted intervention. Sulindac and Celecoxib were observed to be efficient in reducing the localized inflammatory condition of colorectal adenocarcinoma along with their role as angiostatic molecules. Molecular docking experiments performed with these NSAIDs could further help in designing more potent and target molecules which might serve as promising chemotherapeutic agents in future.

Acknowledgments We thank Mrs. Bhupinder Kaur, CSIC, PGIMER, Chandigarh for her kind help in acquiring FACS data. Financial assistance from the Department of Biotechnology, Govt. of India (BT/PR11516/MED/30/147/2008) is gratefully acknowledged. We are thankful to University Grants Commission (UGC), Govt. of India for providing fellowship to the research student, Mr. Vivek Vaish. We also acknowledge the contributions of Dr. Ravi Kumar, Application Specialist, Schrödinger, INDIA for kind support in getting trial license for Schrödinger Suit 2011 and help in performing the docking studies.

Conflict of interest The authors declare no conflict of interest.

References

1. Kundu, J. K., & Surh, Y. J. (2008). Inflammation: Gearing the journey to cancer. *Mutation Research,659*, 15–30. doi:10.1016/j.mrrev.2008.03.002.
2. Klenke, F. M., Gebhard, M. M., Ewerbeck, V., Abdollahi, A., Huber, P. E., & Sckell, A. (2006). The selective Cox-2 inhibitor Celecoxib suppresses angiogenesis and growth of secondary bone tumors: An intravital microscopy study in mice. *BMC Cancer,12*(6), 9. doi:10.1186/1471-2407-6-9.
3. Aggarwal, B. B., Shishodia, S., Sandur, S. K., Pandey, M. K., & Sethi, G. (2006). Inflammation and cancer: How hot is the link? *Biochemical Pharmacology,72*, 1605–1621. doi:10.1016/j.bcp.2006.06.029.
4. Inaba, T., Sano, H., Kawahito, Y., Hla, T., Akita, K., Toda, M., et al. (2003). Induction of cyclooxygenase-2 in monocyte/macrophage by mucins secreted from colon cancer cells. *Proceedings of the National Academy of Sciences of the United States of America,100*, 2736–2741.
5. Solà-Villà, D., Camacho, M., Solà, R., Soler, M., Diaz, J. M., & Vila, L. (2006). IL-1beta induces VEGF, independently of PGE2 induction, mainly through the PI3-K/mTOR pathway in renal mesangial cells. *Kidney International,70*, 1935–1941. doi:10.1038/sj.ki.5001948.
6. Liu, W., Reinmuth, N., Stoeltzing, O., Parikh, A. A., Tellez, C., Williams, S., et al. (2003). Cyclooxygenase-2 is up-regulated by interleukin-1 beta in human colorectal cancer cells via multiple signaling pathways. *Cancer Research,63*, 3632–3636.
7. Maihöfner, C., Charalambous, M. P., Bhambra, U., Lightfoot, T., Geisslinger, G., Gooderham, N. J., et al. (2003). Expression of cyclooxygenase-2 parallels expression of interleukin-1beta, interleukin-6 and NF-kappaB in human colorectal cancer. *Carcinogenesis,24*, 665–671. doi:10.1093/carcin/bgg006.
8. Zhang, M., Yao, Z., Dubois, S., Ju, W., Müller, J. R., & Waldmann, T. A. (2009). Interleukin-15 combined with an anti-CD40 antibody provides enhanced therapeutic efficacy for murine models of colon cancer. *Proceedings of the National Academy of Sciences of the United States of America,106*, 7513–7518.
9. Wu, Y., & Zhou, B. P. (2009). Inflammation: A driving force speeds cancer metastasis. *Cell Cycle,8*, 3267–3273.
10. Kaur, J., & Sanyal, S. N. (2011). Diclofenac, a selective COX-2 inhibitor, inhibits DMH-induced colon tumorigenesis through suppression of MCP-1, MIP-1α and VEGF. *Molecular Carcinogenesis,50*, 707–718. doi:10.1002/mc.20736.
11. Jana, N. R. (2008). NSAIDs and apoptosis. *Cellular and Molecular Life Sciences,65*, 1295–1301. doi:10.1007/s00018-008-7511-x.
12. Vaish, V., Tanwar, L., Kaur, J., & Sanyal, S. N. (2011). Chemopreventive effects of non-steroidal anti-inflammatory drugs in early neoplasm of experimental colorectal cancer: An apoptosome study. *Journal of Gastrointestinal Cancer,42*, 195–203.
13. Vaish, V., Tanwar, L., & Sanyal, S. N. (2010). The role of NF-κB and PPARγ in experimentally induced colorectal cancer and chemoprevention by cyclooxygenase-2 inhibitors. *Tumour Biology,31*, 427–436.
14. Vaish, V., & Sanyal, S. N. (2011). Chemopreventive effects of NSAIDs on cytokines and transcription factors during the early stages of colorectal cancer. *Pharmacological Reports,63*, 1210–1221.
15. Vaish, V., & Sanyal, S. N. (2011). Non steroidal anti-inflammatory drugs modulate the physicochemical properties of plasma membrane in experimental colorectal cancer: A fluorescence spectroscopic study. *Molecular and Cellular Biochemistry,358*, 161–171.
16. Brown, W. A., Skinner, S. A., Malcontenti-Wilson, C., Vogiagis, D., & O'Brien, P. E. (2001). Non-steroidal anti-inflammatory drugs with activity against either cyclooxygenase 1 or cyclooxygenase 2 inhibit colorectal cancer in a DMH rodent model by inducing apoptosis and inhibiting cell proliferation. *Gut,48*, 660–666.
17. Mouillé, B., Robert, V., & Blachier, F. (2004). Adaptative increase of ornithine production and decrease of ammonia metabolism in rat colonocytes after hyperproteic diet ingestion. *American Journal of Physiology. Gastrointestinal and Liver Physiology,287*, G344–G351.
18. Bradford, M. M. (1976). A rapid and sensitive method for the quantitation of microgram quantities of protein utilizing the principle of protein–dye binding. *Analytical Biochemistry,72*, 248–254.
19. Billings, P. C., Habres, J. M., Liao, D. C., & Tuttle, S. W. (1991). Human fibroblasts contain a proteolytic activity which is inhibited by the Bowman–Birk protease inhibitor. *Cancer Research,51*, 5539–5543.
20. Stuehr, D. J., & Marletta, M. A. (1987). Synthesis of nitrite and nitrate in murine macrophage cell lines. *Cancer Research,47*, 5590–5594.

21. Boyde, T. R., & Rahmatullah, M. (1980). Optimization of conditions for the colorimetric determination of citrulline, using diacetyl monoxime. *Analytical Biochemistry,107*, 424–431.
22. Piccagli, L., Fabbri, E., Borgatti, M., Bezzerri, V., Mancini, I., Nicolis, E., et al. (2008). Docking of molecules identified in bioactive medicinal plants extracts into the p50 NF-kappaB transcription factor: Correlation with inhibition of NF-kappaB/DNA interactions and inhibitory effects on IL-8 gene expression. *BMC Structural Biology,3*(8), 38.
23. Friesner, R. A., Banks, J. L., Murphy, R. B., Halgren, T. A., Klicic, J. J., Mainz, D. T., et al. (2004). Glide: A new approach for rapid, accurate docking and scoring. 1. Method and assessment of docking accuracy. *Journal of Medicinal Chemistry,47*, 1739–1749.
24. Friesner, R. A., Murphy, R. B., Repasky, M. P., Frye, L. L., Greenwood, J. R., Halgren, T. A., et al. (2006). Extra precision glide: Docking and scoring incorporating a model of hydrophobic enclosure for protein-ligand complexes. *Journal of Medicinal Chemistry,49*, 6177–6196.
25. Balkwill, F., & Mantovani, A. (2001). Inflammation and cancer: Back to Virchow? *Lancet,357*, 539–545.
26. Vigers, G. P., Dripps, D. J., Edwards, C. K, 3rd, & Brandhuber, B. J. (2000). X-ray crystal structure of a small antagonist peptide bound to interleukin-1 receptor type 1. *Journal of Biological Chemistry,275*, 36927–36933. doi:10.1074/jbc.M006071200.
27. Saijo, Y., Tanaka, M., Miki, M., Usui, K., Suzuki, T., Maemondo, M., et al. (2002). Proinflammatory cytokine IL-1 beta promotes tumor growth of Lewis lung carcinoma by induction of angiogenic factors: In vivo analysis of tumor–stromal interaction. *Journal of Immunology,169*, 469–475.
28. Yang, X. Y., Wang, L. H., Mihalic, K., Xiao, W., Chen, T., Li, P., et al. (2002). Interleukin (IL)-4 indirectly suppresses IL-2 production by human T lymphocytes via peroxisome proliferator-activated receptor gamma activated by macrophage-derived 12/15-lipoxygenase ligands. *Journal of Biological Chemistry,277*, 3973–3978.
29. Yang, X. Y., Wang, L. H., & Farrar, W. L. (2008). A role for PPARgamma in the regulation of cytokines in immune cells and cancer. *PPAR Research,2008*, 961753.
30. Cornejo, M. G., Boggon, T. J., & Mercher, T. (2009). JAK3: A two-faced player in hematological disorders. *International Journal of Biochemistry & Cell Biology,41*, 2376–2379.
31. Kirken, R. A., Rui, H., Malabarba, M. G., Howard, O. M., Kawamura, M., O'Shea, J. J., et al. (1995). Activation of JAK3, but not JAK1, is critical for IL-2-induced proliferation and STAT5 recruitment by a COOH-terminal region of the IL-2 receptor beta-chain. *Cytokine,7*, 689–700.
32. Lin, Q., Lai, R., Chirieac, L. R., Li, C., Thomazy, V. A., Grammatikakis, I., et al. (2005). Constitutive activation of JAK3/STAT3 in colon carcinoma tumors and cell lines: Inhibition of JAK3/STAT3 signaling induces apoptosis and cell cycle arrest of colon carcinoma cells. *American Journal of Pathology,167*, 969–980.
33. Tsareva, S. A., Moriggl, R., Corvinus, F. M., Wiederanders, B., Schütz, A., Kovacic, B., et al. (2007). Signal transducer and activator of transcription 3 activation promotes invasive growth of colon carcinomas through matrix metalloproteinase induction. *Neoplasia,9*, 279–291.
34. Mora, L. B., Buettner, R., Seigne, J., Diaz, J., Ahmad, N., Garcia, R., et al. (2002). Constitutive activation of Stat3 in human prostate tumors and cell lines: Direct inhibition of Stat3 signaling induces apoptosis of prostate cancer cells. *Cancer Research,62*, 6659–6666.
35. Bill, M. A., Fuchs, J. R., Li, C., Yui, J., Bakan, C., Benson, D. M, Jr, et al. (2010). The small molecule curcumin analog FLLL32 induces apoptosis in melanoma cells via STAT3 inhibition and retains the cellular response to cytokines with anti-tumor activity. *Molecular Cancer,25*(9), 165.
36. Sudbeck, E. A., Liu, X. P., Narla, R. K., Mahajan, S., Ghosh, S., Mao, C., et al. (1999). Structure-based design of specific inhibitors of Janus kinase 3 as apoptosis-inducing antileukemic agents. *Clinical Cancer Research,5*, 1569–1582.
37. Siddiquee, K., Zhang, S., Guida, W. C., Blaskovich, M. A., Greedy, B., Lawrence, H. R., et al. (2007). Selective chemical probe inhibitor of Stat3, identified through structure-based virtual screening, induces antitumor activity. *Proceedings of the National Academy of Sciences of the United States of America,104*, 7391–7396. doi:10.1073_pnas.0609757104.
38. Rath, P. C., & Aggarwal, B. B. (1999). TNF-induced signaling in apoptosis. *Journal of Clinical Immunology,19*, 350–364.
39. Yasui, H., Adachi, M., & Imai, K. (2003). Combination of tumor necrosis factor-alpha with Sulindac augments its apoptotic potential and suppresses tumor growth of human carcinoma cells in nude mice. *Cancer,97*, 1412–1420.
40. Onizawa, M., Nagaishi, T., Kanai, T., Nagano, K., Oshima, S., Nemoto, Y., et al. (2009). Signaling pathway via TNF-alpha/NF-kappaB in intestinal epithelial cells may be directly involved in colitis-associated carcinogenesis. *American Journal of Physiology. Gastrointestinal and Liver Physiology,296*, G850–G859.
41. Takenouchi-Ohkubo, N., Moro, I., Mukae, S., Kaneko, Y., & Komiyama, K. (2008). Tumour necrosis factor-alpha-mediated human polymeric immunoglobulin receptor expression is regulated by both mitogen-activated protein kinase and phosphatidylinositol-3-kinase in HT-29 cell line. *Immunology,123*, 500–507.
42. Zhou, A., Scoggin, S., Gaynor, R. B., & Williams, N. S. (2003). Identification of NF-kappa B-regulated genes induced by TNF-alpha utilizing expression profiling and RNA interference. *Oncogene,22*, 2054–2064.
43. Remels, A. H., Langen, R. C., Gosker, H. R., Russell, A. P., Spaapen, F., Voncken, J. W., et al. (2009). PPARgamma inhibits NF-kappaB-dependent transcriptional activation in skeletal muscle. *American Journal of Physiology—Endocrinology and Metabolism,297*, E174–E183.
44. Takada, I., Suzawa, M., & Kato, S. (2005). Nuclear receptors as targets for drug development: Crosstalk between peroxisome proliferator-activated receptor gamma and cytokines in bone marrow-derived mesenchymal stem cells. *Journal of Pharmacological Science,97*, 184–189.
45. Nam, K. S., Kim, M. K., & Shon, Y. H. (2007). Inhibition of proinflammatory cytokine-induced invasiveness of HT-29 cells by chitosan oligosaccharide. *Journal of Microbiology and Biotechnology,17*, 2042–2045.
46. Cianchi, F., Cortesini, C., Fantappiè, O., Messerini, L., Schiavone, N., Vannacci, A., et al. (2003). Inducible nitric oxide synthase expression in human colorectal cancer: Correlation with tumor angiogenesis. *American Journal of Pathology,162*, 793–801.
47. Fukumura, D., Gohongi, T., Kadambi, A., Izumi, Y., Ang, J., Yun, C. O., et al. (2001). Predominant role of endothelial nitric oxide synthase in vascular endothelial growth factor-induced angiogenesis and vascular permeability. *Proceedings of the National Academy of Sciences of the United States of America,98*, 2604–2609.
48. Song, Z. J., Gong, P., & Wu, Y. E. (2002). Relationship between the expression of iNOS, VEGF, tumor angiogenesis and gastric cancer. *World Journal of Gastroenterology,8*, 591–595.
49. Rosenfeld, R. J., Bonaventura, J., Szymczyna, B. R., MacCoss, M. J., Arvai, A. S., Yates, J. R, I. I. I., et al. (2010). Nitric-oxide synthase forms N-NO-pterin and S-NO-cys: Implications for activity, allostery, and regulation. *Journal of Biological Chemistry,285*, 31581–31589.
50. Hong, K. H., Ryu, J., & Han, K. H. (2005). Monocyte chemoattractant protein-1-induced angiogenesis is mediated by vascular endothelial growth factor-A. *Blood,105*, 1405–1407.
51. Luo, X., Yu, Y., Liang, A., Xie, Y., Liu, S., Guo, J., et al. (2004). Intratumoral expression of MIP-1β induces antitumor responses

in a pre-established tumor model through chemoattracting T cells and NK cells. *Cellular & Molecular Immunology,1*, 199–204.
52. Hoeben, A., Landuyt, B., Highley, M. S., Wildiers, H., Van Oosterom, A. T., & De Bruijn, E. A. (2004). Vascular endothelial growth factor and angiogenesis. *Pharmacological Reviews,56*, 549–580.
53. Harris, P. A., Cheung, M., Hunter, R. N, I. I. I., Brown, M. L., Veal, J. M., Nolte, R. T., et al. (2005). Discovery and evaluation of 2-anilino-5-aryloxazoles as a novel class of VEGFR2 kinase inhibitors. *Journal of Medicinal Chemistry,48*, 1610–1619.
54. Sternlicht, M. D., & Werb, Z. (2001). How matrix metalloproteinases regulate cell behavior. *Annual Review of Cell and Developmental Biology,17*, 463–516.
55. Page-McCaw, A., Ewald, A. J., & Werb, Z. (2007). Matrix metalloproteinases and the regulation of tissue remodelling. *Nature Reviews Molecular Cell Biology,8*, 221–233.